Thermochemistry and Electronic Structure of Small Boron Clusters (B n , n = 5−13) and Their Anions

ARTICLE *in* THE JOURNAL OF PHYSICAL CHEMISTRY A · DECEMBER 2009

Impact Factor: 2.69 · DOI: 10.1021/jp9085848 · Source: PubMed

4 AUTHORS, INCLUDING:

Truong Tai
University of Leuven
65 PUBLICATIONS **498** CITATIONS
SEE PROFILE

Minh Tho Nguyen
University of Leuven
747 PUBLICATIONS **10,762** CITATIONS
SEE PROFILE

David A Dixon
University of Alabama
765 PUBLICATIONS **21,986** CITATIONS
SEE PROFILE

Thermochemistry and Electronic Structure of Small Boron Clusters (B_n, $n = 5-13$) and Their Anions

Truong Ba Tai,[†] Daniel J. Grant,[‡] Minh Tho Nguyen,*[,†,‡] and David A. Dixon*[,‡]

Department of Chemistry, and Mathematical Modeling and Computational Science Center (LMCC), Katholieke Universiteit Leuven, B-3001 Leuven, Belgium, and Department of Chemistry, The University of Alabama, Shelby Hall, Box 870336, Tuscaloosa, Alabama 35847-0336

Received: September 4, 2009; Revised Manuscript Received: October 27, 2009

Thermochemical parameters of a set of small-sized neutral (B_n) and anionic (B_n^-) boron clusters, with $n = 5-13$, were determined using coupled-cluster theory CCSD(T) calculations with the aug-cc-pV*n*Z (n = D, T, and Q) basis sets extrapolated to the complete basis set limit (CBS) plus addition corrections and/or G3B3 calculations. Enthalpies of formation, adiabatic electron affinities (EA), vertical (VDE), and adiabatic (ADE) detachment energies were evaluated. Our calculated EAs are in good agreement with recent experiments (values in eV): B_5 (CBS, 2.29; G3B3, 2.48; exptl., 2.33 ± 0.02), B_6 (CBS, 2.59; G3B3, 3.23; exptl., 3.01 ± 0.04), B_7 (CBS, 2.62; G3B3, 2.67; exptl., 2.55 ± 0.05), B_8 (CBS, 3.02; G3B3, 3.11; exptl., 3.02 ± 0.02), B_9 (G3B3, 3.03; exptl., 3.39 ± 0.06), B_{10} (G3B3, 2.85; exptl., 2.88 ± 0.09), B_{11} (G3B4, 3.48;, exptl., 3.43 ± 0.01), B_{12} (G3B3, 2.33; exptl., 2.21 ± 0.04), and B_{13} (G3B3, 3.62; exptl., 3.78 ± 0.02). The difference between the calculated adiabatic electron affinity and the adiabatic detachment energy for B_6 is due to the fact that the geometry of the anion is not that of the ground-state neutral. The calculated adiabatic detachment energies to the ^3A_u, C_{2h} and ^1A_g, D_{2h} excited states of B_6, which have geometries similar to the ^1A_g, D_{2h} state of B_6^-, are 2.93 and 3.06 eV, in excellent agreement with experiment. The VDEs were also well reproduced by the calculations. Partitioning of the electron localization functions into π and σ components allows probing of the partial and local delocalization in global nonaromatic systems. The larger clusters appear to exhibit multiple aromaticity. The binding energies per atom vary in a parallel manner for both neutral and anionic series and approach the experimental value for the heat of atomization of B. The resonance energies and the normalized resonance energies are convenient indices to quantify the stabilization of a cluster of elements.

Introduction

Boron clusters have a wide range of properties and have been characterized by a number of experimental techniques including mass spectrometry.[1] Experimental and theoretical studies on the electronic structure,[2−5] chemical bonding,[6−8] and spectroscopic properties[9−15] of bare boron clusters as well as doped boron clusters[16−20] have been reported. Similar to carbon-based materials, boron nanotubes (and fullerenes, if synthesized) have been considered as potential materials for hydrogen storage.[21] Recent findings on novel properties of boron-based nanotubular materials[22,23] are stimulating further studies on the small-sized gas-phase clusters to determine their fundamental properties and growth patterns.

There are a substantial number of computational studies of boron clusters, and we describe some here. Boustani[24] predicted that, for the small boron clusters, the quasi-planar and planar structures are more stable than the three-dimensional structures, and this result was confirmed by subsequent theoretical and experimental studies. Wang, Boldyrev, and co-workers[25−28] used photoelectron spectroscopy (PES) in combination with quantum chemical calculations to investigate the structural and electronic properties of a series of boron cluster anions B_n^- ($n = 3-20$) and proposed that the planarity and quasi-planarity of boron clusters is due to a delocalization of the π-electrons in 2D structures. They also suggested that the π-electron delocalization in B_n follows the Hückel model for aromaticity and antiaromaticity as found in cyclic hydrocarbons. In contrast, Aihara and co-workers[29] analyzed the structure of boron clusters in terms of topological resonance (TRE) arguments and concluded that their aromaticity is not related to the total number of π-electrons, and the Hückel rule can therefore not be applied. Subsequently, Zubarev and Boldyrev[6] reexamined the chemical bonding of B_n clusters using natural bond orbitals (NBO), canonical molecular orbitals (MOs), and nuclear independent chemical shift (NICS) and predicted that the globally delocalized π or σ MOs in boron clusters exhibit both aromatic and antiromatic characters following the Hückel rule. These authors also showed that the presence of islands of π-aromaticity in a globally π-antiaromatic molecule results in higher structural stability.

We recently predicted the heats of formation of the global energy minimum structures of a series of small boron B_n, boron oxide B_nO_m clusters, and their anions, with $n \leq 4$, using high accuracy quantum chemical methods.[30] In addition, we analyzed their electronic structure in terms of the topology of electron localization function (ELF) and molecular orbitals. We now extend the calculations and analyses to the larger boron clusters B_n and their anions B_n^-, with $n = 5-13$. In view of the lack of reliable thermochemical parameters, we first predict their heats of formation. Subsequently, we analyze the bonding of the clusters, in particular the questions related to their electronic structure.

* Corresponding author. E-mail: dadixon@bama.ua.edu (D.A.D.); minh.nguyen@chem.kuleuven.be (M.T.N.).
[†] Katholieke Universiteit Leuven.
[‡] The University of Alabama.

10.1021/jp9085848
Published on Web 12/11/2009

Computational Methods

All quantum chemical calculations were carried out using the Gaussian 03[31] and Molpro 2006[32] suites of programs. Enthalpies of formation of the B_n and B_n^- clusters were evaluated from the corresponding total atomization energies (TAE).[33] Two sets of calculations were performed. For $n = 5-9$, the complete basis set (CBS) approach previously used for the series of $n = 2-4$[30] and the G3B3 approach[34] were used. The G3B3 (G3/B3LYP) approach is a composite technique in which a sequence of ab initio density functional theory and molecular orbital calculations is performed to obtain the total energy of a given molecular species. Because a G3B3 calculation is computationally less demanding than a CBS counterpart, we used only the G3B3 approach for the larger B_n clusters with $n = 10-13$.

We briefly describe the CBS approach. Geometry parameters were fully optimized at the second-order perturbation theory (MP2) level with the correlation consistent aug-cc-pVDZ and aug-cc-pVTZ basis sets. The fully unrestricted formalism (UHF, UMP2) was used for open-shell system calculations done with Gaussian 03. The valence electronic energies were computed using coupled-cluster CCSD(T) theory[35] extrapolated to the complete basis set limit (CBS) using the correlation-consistent basis sets.[36] The single-point electronic energies were calculated by using the restricted coupled-cluster R/UCCSD(T) formalism[37−39] in conjunction with the correlation-consistent aug-cc-pVnZ (n = D, T, and Q) basis sets at the (U)MP2/aug-cc-pVDZ or (U)MP2/aug-cc-pVTZ optimized geometries with the Molpro program. For simplicity, the basis sets are labeled as aVnZ. The CCSD(T) energies were extrapolated to the CBS limit energies using expression 1:[40]

$$E(x) = A_{\mathrm{CBS}} + B\exp[-(x-1)] + C\exp[-(x-1)^2] \quad (1)$$

where $x = 2$, 3, and 4 for the aVnZ basis D, T, and Q, respectively (total CCSD(T) electronic energies as a function of basis set are given in Table S1 of the Supporting Information). The zero-point energies (ZPE) were calculated from harmonic vibrational frequencies at the MP2/aVDZ level and are given in Table S2. Additional smaller corrections were included in the TAE calculations. Core−valence corrections (ΔE_{CV}) were obtained at the CCSD(T)/cc-pwCVTZ level of theory with Molpro.[41] Douglas−Kroll−Hess (DKH) scalar relativistic corrections ($\Delta E_{\mathrm{DKH\text{-}SR}}$), which account for changes in the relativistic contributions to the total energies of the molecule and the constituent atoms, were calculated using the spin-free, one-electron DKH Hamiltonian with Molpro.[42−44] $\Delta E_{\mathrm{DKH\text{-}SR}}$ is defined as the difference in the atomization energy between the results obtained from basis sets recontracted for DKH calculations[43] and the atomization energy obtained with the normal valence basis set of the same quality. The DKH calculations were obtained as the differences of the results from the CCSD(T)/cc-pVTZ and the CCSD(T)/cc-pVTZ-DK levels of theory. Finally, a spin−orbit (SO) correction of 0.03 kcal/mol for the B atom obtained from the excitation energies of Moore[45] is used. The total atomization energy ($\sum D_0$ or TAE) of a compound is given by eq 2:

$$\sum D_0 = \Delta E_{\mathrm{elec}}(\mathrm{CBS}) + \Delta E_{\mathrm{CV}} + \Delta E_{\mathrm{DKH\text{-}SR}} + \Delta E_{\mathrm{SO}} - \Delta E_{\mathrm{ZPE}} \quad (2)$$

By combining our computed $\sum D_0$ values from either the CBS or the G3B3 calculations, with the known heat of formation at 0 K for the element B, we can derive ΔH_f° values at 0 K for the molecules in the gas phase. In this work, we used the value of $\Delta H_f^\circ(\mathrm{B}) = 135.1 \pm 0.2$ kcal/mol,[46] and the rationale for this selection was discussed in our previous work.[30] We obtain heats of formation at 298 K by following the procedures outlined by Curtiss et al.[47] We use the calculated heats of formation at 0 K to evaluate the electron affinities and other energetic quantities.[30,48]

The analysis of chemical bonding phenomenon was performed using the electron localization function (ELF)[49] supplemented by analyses of topological bifurcation[50] and canonical MOs. The ELF is a local measure of the Pauli repulsion between electrons owing to the exclusion principle in 3D space. The definition of ELF, $\eta(\mathbf{r})$, is given by following eq 3:

$$\begin{aligned} \eta(\mathbf{r}) &= \frac{1}{1 + (D_{\mathrm{P}}/D_{\mathrm{h}})^2} \\ D_{\mathrm{P}} &= \frac{1}{2}\sum_{i=1}^{N}|\nabla\psi_i|^2 - \frac{1}{8}\frac{|\nabla\rho|^2}{\rho} \\ D_{\mathrm{h}} &= \frac{3}{10}(3\pi^2)^{2/3}\rho^{5/3} \\ \rho &= \sum_{i=1}^{N}|\psi_i(\mathbf{r})|^2 \end{aligned} \quad (3)$$

where D_{P} and D_{h} are the local kinetic energy density due to the Pauli exclusion principle and the Thomas−Fermi kinetic energy density, respectively, and ρ is the electron density. These quantities can be evaluated using either Hartree−Fock or Koln−Sham orbitals. The total ELF can then be partitioned in terms of separate ELF_σ and ELF_π components. The latter can be used as indices describing the aromaticity of cyclic molecules.[51] A π and σ aromatic ring possesses a high bifurcation value of ELF_π and ELF_σ, whereas the corresponding bifurcation value in an antiaromatic system is very low. The density for the ELF analysis of the lowest-energy state in each spin manifold was obtained at the (U)B3LYP/6-311+G(d) level. The total ELF was mapped out using the TOPMOD software,[52] whereas the ELF_π and ELF_σ were constructed using the DGrid-4.2 software.[53] All isosurfaces of the ELF, ELF_π, and ELF_σ have been plotted using the Gopenmol software.[54]

Results and Discussion

The shapes of the equilibrium structures of the B_n and B_n^- clusters are shown in Figures 1 ($n = 5-8$) and 2 ($n = 9-13$). These include for each cluster the global energy minimum and selected lower-lying isomers. To simplify the presentation of data, the ELF isosurfaces with one bifurcation value are also displayed in these figures. The total G3B3 energies as well as the corresponding $\sum D_0$ values are summarized in Table S3 of the Supporting Information. The optimized geometries of the lowest-lying isomers using the B3LYP/6-31G(d) method (within the G3B3 approach) are listed in Table S4. The different components obtained in the CBS protocol to predict the total atomization energies ($\sum D_0$) and the $\sum D_0$ of B_n and B_n^-, with $n = 5-9$ (except for B_9), are given in Table 1. The heats of formation of the clusters derived using the $\sum D_0$ obtained from both CBS and G3B3 methods are given in Table 2. The adiabatic electron affinities (EAs) of the neutrals B_n are given in Table 3, and the vertical detachment energies (VDEs) of the B_n^- anions computed using the single-point G3B3 and CBS methods are

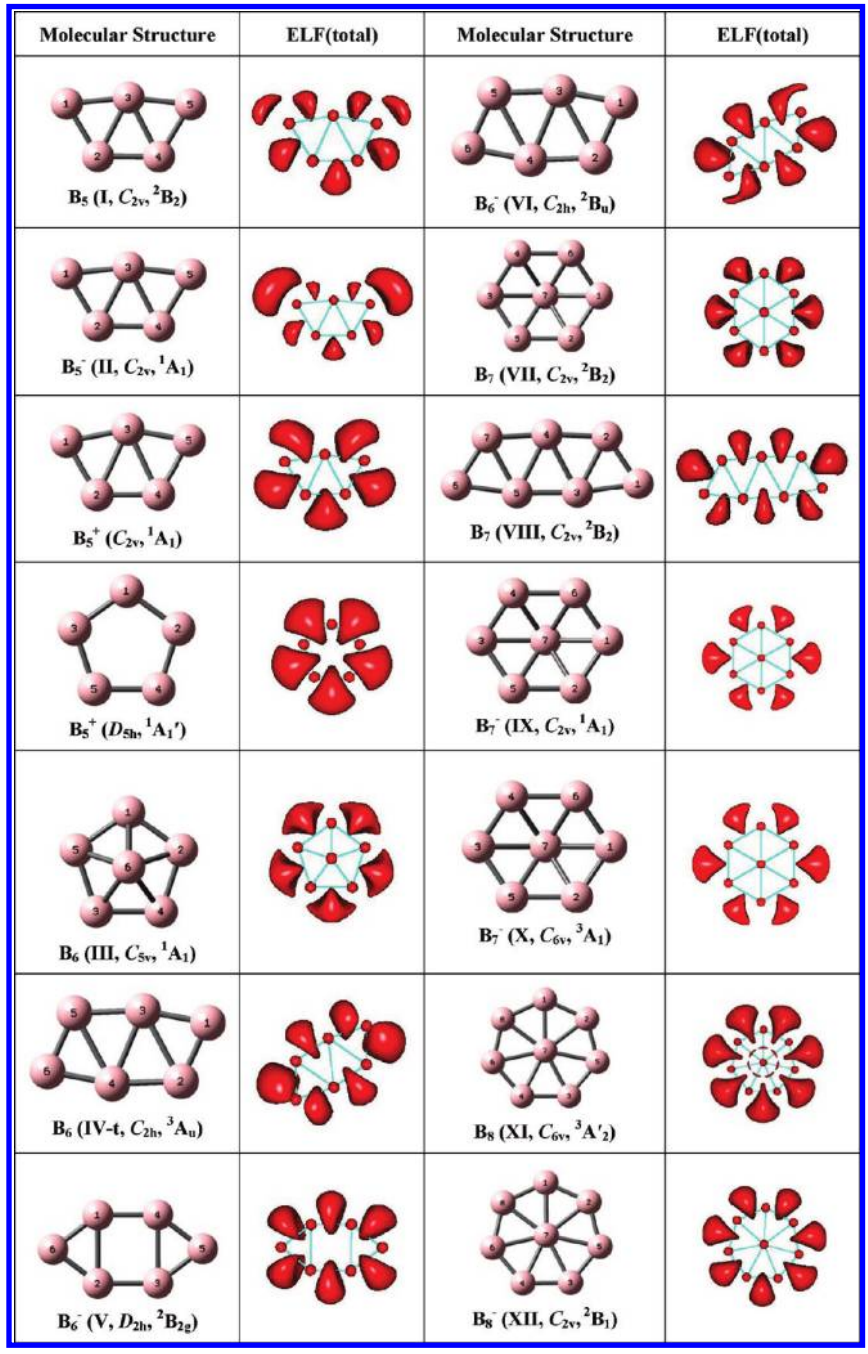

Figure 1. Shape of the lowest-energy structures of B_n and B_n^- ($n = 5-8$) and their ELF localization domains.

given in Table 4. The dependence of the singlet−triplet gaps with respect to the basis set is given in Table 5.

The heats of formation of B_2, B_3, and B_4 and their anions were determined in our previous work at the CBS level and compared to previous experimental and theoretical results.[30] For purposes of comparison, both the CBS and the G3B3 values for these clusters are also listed in Table 2. We note that the G3B3 value of 206.0 kcal/mol for ΔH_f at 298 K of B_2 ($^3\Sigma_g^-$) is close to the CBS result of 207.4 kcal/mol, and both are at the high end of the range of the experimental value of 198.3 ± 8.0 kcal/mol.[55] For B_3 ($^2A_1'$) and B_4 (^1A_g), the respective G3B3 values of 211.5 and 228.5 kcal/mol are consistent with the respective CBS values of 211.7 and 226.4 kcal/mol.[30] For the larger species, the differences between the G3B3 and CBS values vary from 1 to 3 kcal/mol, which reflects the degree of accuracy of the G3B3 results. Different aspects of the geometric and electronic structures of the clusters have been analyzed in detail in numerous previous studies, and thus do not warrant additional comments. We focus the discussion only on the new thermochemical results and analyses of the bonding.

B_5. The B_5 and B_5^- clusters have been extensively studied both experimentally and theoretically. Kato et al.[2] reported that B_5 has either a C_{2v} ($^2A_2$) or a C_2 (^2B) ground state. Boustani,[4] Li and Jin,[56] Boldyrev and co-workers,[6,57] and Ricca et al.[58] reported that the most stable structure of B_5 is a planar C_{2v} $^2B_2$ state. In contrast, Ray et al.[58] as well as Niu et al.[59] suggested a trigonal bipyramid D_{3h} as the lowest energy structure. Our calculations concur with the prediction that the B_5 radical possesses a $^2B_2$ ground state **I** (Figure 1). The high spin state still has a C_{2v} structure ($^4B_2$) and is the second lowest-lying isomer. The quartet−doublet gap is ~43 kcal/mol, which is close to the value of 40 kcal/mol estimated by Alexandrova et al.[25]

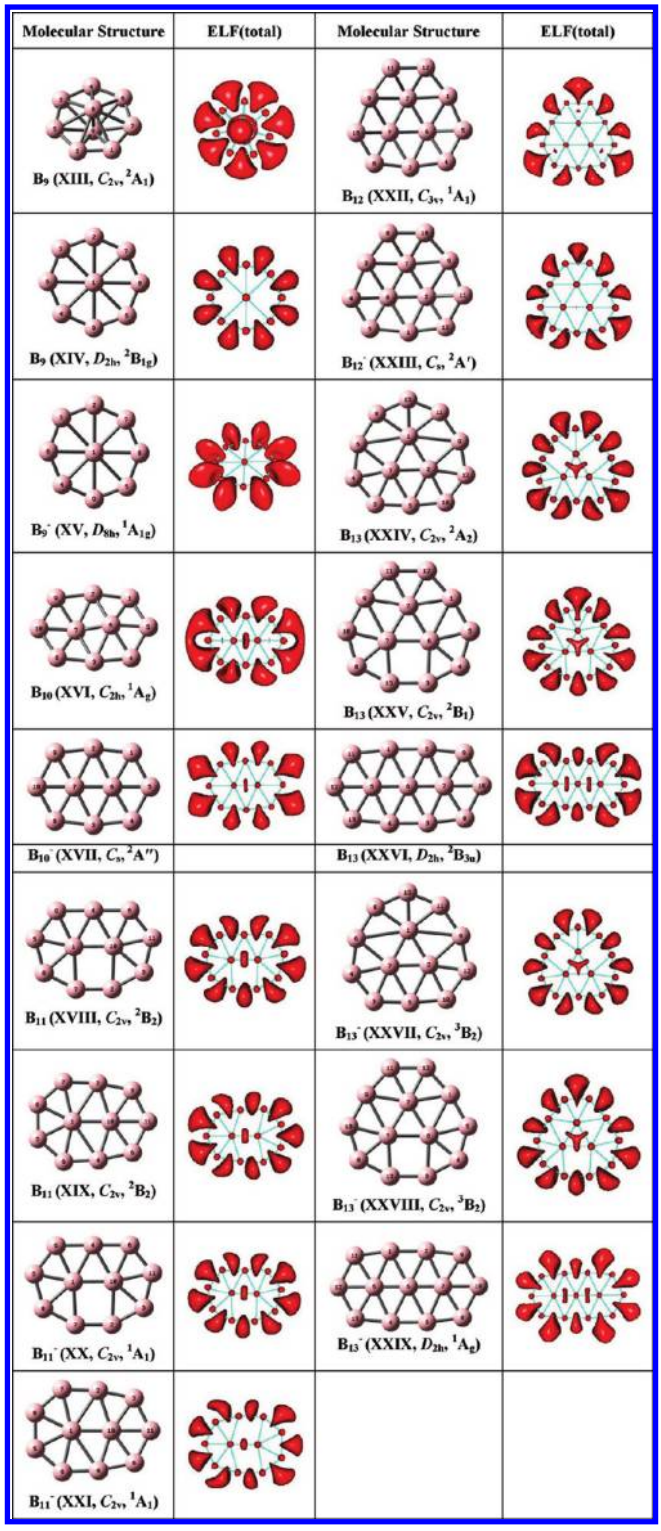

Figure 2. Shape of the lowest-energy structures B_n and B_n^- ($n = 9-13$) and their ELF localization domains.

from GEGA/B3LYP/3-21G calculations. At the B3LYP/6-31G(d) level, a search of the $^2A_1$ state of B_5 led to a nonplanar structure (C_{2v}), which is ~58 kcal/mol higher in energy than **I**. A $\sum D_0$ of 407 kcal/mol for B_5 **I** was reported at the CCSD(T)/6-311+G(2df) + ZPE level,[25] but no corresponding value for the heat of formation was derived.[25] The latter $\sum D_0$ estimate differs significantly from the present values of 420.6 (G3B3) and 423.8 (CBS) kcal/mol.

Attaching one electron to the neutral B_5 ($^2B_2$) does not affect the geometry much, and the closed-shell $^1A_1$ structure is found to be the most stable structure for the B_5^- anion **II** (Figure 1), in agreement with the available theoretical results. The lowest-lying triplet state is distorted by an out-of-plane motion to form a C_2 ^3B structure, and the $^3B-^1A_1$ gap of B_5^- is ~10 kcal/mol (G3B3 and CBS, Table 5), which is larger than that of 5.3 kcal/mol previously obtained by UB3LYP/6-311+G(d) calculations.[25]

TABLE 1: CCSD(T)/CBS Total Atomization Energies ($\sum D_0$ = TAE in kcal/mol) for the Neutral B_n and Anionic B_n^- Boron Clusters ($n = 5-9$) and the Different Components[a]

molecule	ΔCBS[b]	ΔE_{ZPE}[c]	ΔE_{CV}[d]	ΔE_{SR}[e]	ΔE_{SO}[f]	$\sum D_0$(0 K)
B_5 ($^2B_2$, C_{2v}, **I**)	429.67	9.91	4.55	−0.32	−0.15	423.84
B_5^- ($^1A_1$, C_{2v}, **II**)	482.09	9.56	4.61	−0.34	−0.15	476.65
B_5^- (^3B, C_2, **II-t**)	472.19	11.31	4.80	−0.35	−0.15	465.19
B_6 ($^1A_1$, C_{5v}, **III**)	538.89	13.44	6.46	−0.44	−0.18	531.29
B_6 (^3A_u, C_{2h}, **IV-t**)	530.11	11.98	5.82	−0.41	−0.18	523.36
B_6 (^1A_g, D_{2h}, **IV-d**)	526.64	11.35	5.69	−0.38	−0.18	520.42
B_6 (^1A, C_2, **IV-s**)	527.03	11.90	5.48	−0.39	−0.18	520.03
B_6^- ($^2B_{2g}$, D_{2h}, **V**)	597.20	11.84	6.24	−0.42	−0.18	590.99
B_6^- ($^2B_{1u}$, D_{2h}, **V-u**)	585.42	15.78	6.42	−0.43	−0.18	575.45
B_6^- (^2B_u, C_{2h}, **VI**)	592.09	13.55	6.54	−0.44	−0.18	584.46
B_6^- (^2A_u, C_{2h}, **V-c**)	573.27	12.37	5.84	−0.46	−0.18	566.10
B_6^- ($^2A''$, C_s, **V-s**)	582.14	12.78	6.56	−0.47	−0.18	575.28
B_7 ($^2B_2$, C_{2v}, **VII**)	673.37	16.64	7.61	−0.53	−0.21	663.60
B_7^- ($^1A_1$, C_{2v}, **IX**)	732.94	15.79	7.58	−0.56	−0.21	723.96
B_7^- ($^1A_1$, C_{2v}, **IX-a**)	723.92	15.68	7.34	−0.54	−0.21	714.83
B_7^- ($^3A_1$, C_{6v}, **X**)	733.20	17.56	7.85	−0.58	−0.21	722.70
B_8 ($^3A_2'$, D_{7h}, **XI**)	809.68	19.13	8.40	−0.59	−0.24	798.12
B_8^- ($^2B_1$, C_{2v}, **XII**)	878.20	18.32	8.79	−0.61	−0.24	867.82
B_9^- ($^1A_{1g}$, D_{8h}, **XV**)	985.98	19.58	9.47	−0.64	−0.27	974.97
B_9^- ($^3A'$, C_s, **XV-t**)	953.96	19.77	9.75	−0.72	−0.27	942.94

[a] Atomic asymptotes calculated with the R/UCCSD(T) method. [b] Extrapolated by using eq 1 with the aVDZ, aVTZ, and aVQZ basis sets. [c] Zero-point energies taken as 0.5, the sum of the MP2 harmonic frequencies. [d] Core−valence corrections obtained with the cc-pwCVTZ basis sets at the optimized CCSD(T) or MP2 geometries. [e] Scalar relativistic correction based on a CCSD(T)-DK/VTZ-DK calculation and is expressed relative to the CCSD(T) result without the DK correction. [f] Correction due to the incorrect treatment of the atomic asymptotes as an average of spin multiplets. Values based on C. Moore's tables, ref 45.

The adiabatic electron affinity (EA) of B_5 calculated from the heats of formation at 0K of **I** ($^2B_2$) and **II** ($^1A_1$) is 2.48 (G3B3) and 2.29 eV (CBS). As compared to the experimental value of 2.33 eV,[57] the G3B3 value is ~0.15 eV too large, and the CBS result is in good agreement as would be expected (Table 3). The difference between the G3B3 calculated VDE of 2.64 eV and the experimental result of 2.40 ± 0.02 eV is slightly larger[57] (Table 4).

The nature of chemical bonding and aromaticity of boron clusters have extensively been studied to explain their planarity and high stability. We add to this effort a topological analysis of the ELF, in combination with MO interactions. The global minimum C_{2v} structure of the B_5 cluster in both the neutral and the anion states can be understood by considering the geometrical distortions from the higher symmetry geometry of the corresponding B_5^+ cation following electron attachment. The LUMO of B_5^+ (D_{5h}, $^1A_1'$) is degenerate. Addition of one or two electrons into these vacant orbitals to obtain B_5 and B_5^-, respectively, is subject in their low spin states to a Jahn−Teller effect whose stabilization leads to a lower symmetry C_{2v} structure. The high spin triplet state of B_5^- arising from the (e^2) occupancy, $^3A_1'$ (D_{5h}), is calculated to be ~87 kcal/mol higher in energy than the singlet **II** at the B3LYP/6-311+G(d) level.

Analysis of the ELF of B_5 and B_5^- shows the existence of a trisynaptic basin B2B3B4 in each state (see Figure 1 for atom

TABLE 2: Calculated Heats of Formation (ΔH_f at 0 and 298 K, kcal/mol) of the Neutral B_n and Anionic B_n^- Boron Clusters ($n = 5-13$) Using CCSD(T)/CBS and G3B3 Approaches

		ΔH_f(0 K)		ΔH_f(298 K)	
structure (state)	label symmetry	G3B3	CBS	G3B3	CBS
B_2 ($^3\Sigma_g^-$)	$D_{\infty h}$	204.5	205.9	206.0	207.4[a]
B_2^- ($^4\Sigma_g^-$)	$D_{\infty h}$	159.1	160.9	160.6	162.4[a]
B_3 ($^2A_1'$)	D_{3h}	209.9	210.1	211.5	211.7
B_3^- ($^1A_1'$)	D_{3h}	142.7	143.7	144.3	145.3
B_4 (^1A_g)	D_{2h}	226.7	224.6	228.5	226.4
B_4^- ($^2B_{1u}$)	D_{2h}	188.2	185.8	189.8	187.5
B_5 ($^2B_2$)	**I** C_{2v}	254.9	251.7	256.8	253.5
B_5^- ($^1A_1$)	**II** C_{2v}	197.8	198.9	199.6	200.7
B_5^- (^3B)	**II-t** C_2		210.3		211.9
B_6 ($^1A_1$)	**III** C_{5v}	285.2	279.3	286.9	280.9
B_6 (^3A_u)	**IV-t** C_{2h}	291.4	287.2	293.1	289.5
B_6 (^1A_g)	**IV-d** D_{2h}		290.2		291.8
B_6 (^1A)	**IV-s** C_2		290.6		292.8
B_6^- ($^2B_{2g}$)	**V** D_{2h}	210.8	219.6	213.0	220.8
B_6^- ($^2B_{1u}$)	**V-u** D_{2h}		235.1		236.5
B_6^- (^2B_u)	**VI** C_{2h}	234.9	226.1	237.1	228.2
B_6^- (^2A_u)	**V-c** C_{2h}		244.5		246.6
B_6^- ($^2A''$)	**V-s** C_s		235.3		236.7
B_7 ($^2B_2$)	**VII** C_{2v}	286.5	282.1	288.3	284.0
B_7 ($^2B_2$)	**VIII** C_{2v}	313.1		315.1	
B_7^- ($^1A_1$)	**IX** C_{2v}	223.8	221.7	225.6	223.5
B_7^- ($^1A_1$)	**IX-a** C_{2v}		230.9		232.9
B_7^- ($^3A_1$)	**X** C_{6v}	224.9	223.0	226.4	224.5
B_8 ($^3A_2'$)	**XI** D_{7h}	285.3	282.7	287.5	284.8
B_8^- ($^2B_1$)	**XII** C_{2v}	213.5	213.0	216.0	215.3
B_9 ($^2A_1$)	**XIII** C_{2v}	311.9		315.0	
B_9 ($^2B_{1g}$)	**XIV** C_{2v}	323.2		327.0	
B_9^- ($^1A_{1g}$)	**XV** D_{8h}	242.0	240.9	245.3	244.3
B_9^- ($^3A'$)	**XV-t** C_s		273.0		275.6
B_{10} (^1A_g)	**XVI** C_{2h}	312.7		314.8	
B_{10}^- ($^2A''$)	**XVII** C_s	247.0		249.3	
B_{11} ($^2B_2$)	**XVIII** C_{2v}	333.1		336.0	
B_{11} ($^2B_2$)	**XIX** C_{2v}	343.7		346.4	
B_{11}^- ($^1A_1$)	**XX** C_{2v}	252.9		255.7	
B_{11}^- ($^1A_1$)	**XXI** C_{2v}	253.2		255.6	
B_{12} ($^1A_1$)	**XXII** C_{3v}	333.3		335.7	
B_{12}^- ($^2A'$)	**XXIII** C_s	297.6		282.6	
B_{13} ($^2A_2$)	**XXIV** C_{2v}	369.6		373.1	
B_{13} ($^2B_1$)	**XXV** C_{2v}	369.2		372.4	
B_{13} ($^2B_{3u}$)	**XXVI** D_{2h}	374.2		376.7	
B_{13}^- ($^3B_2$)	**XXVII** C_{2v}	308.5		311.8	
B_{13}^- ($^3B_2$)	**XXVIII** C_{2v}	309.5		312.3	
B_{13}^- (^1A_g)	**XXIX** D_{2h}	285.7		288.3	

[a] Experimental values of 198.3 ± 8.0 (B_2) and 168.5 ± 9.2 (B_2^-) kcal/mol from ref 55.

TABLE 3: Adiabatic Electronic Affinities (EA, eV) of Boron Clusters (B_n, $n = 5-13$) Calculated Using the G3B3 and CCSD(T) Methods[a]

neutral (state)	anion (state)	G3B3	CCSD(T)	exptl.[b]
B_2 ($^3\Sigma_g^-$)	B_2^- ($^4\Sigma_g^-$)	1.97	1.95	1.80
B_3 ($^2A_1'$)	B_3^- ($^1A_1'$)	2.91	2.88	2.82 ± 0.02
B_4 (^1A_g)	B_4^- ($^2B_{1u}$)	1.67	1.68	1.60 ± 0.10
B_5 ($^2B_2$)	B_5^- ($^1A_1$)	2.48	2.29	2.33 ± 0.02
B_6 ($^1A_1$)	B_6^- ($^2B_{2g}$)	3.23 (3.50)[c]	2.59 (2.93)[c]	3.01 ± 0.02
B_7 ($^2B_2$)	B_7^- ($^3A_1$)	2.67	2.56	2.55 ± 0.02
B_7 ($^2B_2$)	B_7^- ($^1A_1$)	2.72	2.62	2.55 ± 0.02
B_8 ($^3A_2'$)	B_8^- ($^2B_1$)	3.11	3.02	3.02 ± 0.02
B_9 ($^2A_1$)	B_9^- ($^1A_{1g}$)	3.03 (3.53)[c]		3.39 ± 0.06
B_{10} (^1A_g)	B_{10}^- ($^2A''$)	2.85		2.88 ± 0.09
B_{11} ($^2B_2$)	B_{11}^- ($^1A_1$)	3.48		3.43 ± 0.02
B_{12} ($^1A_1$)	B_{12}^- ($^2A'$)	2.33		2.21 ± 0.04
B_{13} ($^2A_2$)	B_{13}^- (^1A_g)	3.62 (3.81)[c]		3.78 ± 0.02

[a] Evaluated from calculated enthalpies of formation at 0 K. [b] Experimental values from ref 25 correspond to either EAs or ADEs. [c] ADEs are given in parentheses; see text.

TABLE 4: Vertical Detachment Energies (VDE, eV) of Boron Cluster Anions (B_n^-, $n = 5-13$) Calculated Using the G3B3 and CCSD(T) Methods

anion (state)	neutral (state)	G3B3[a]	CCSD(T)[b]	exptl.[c]
B_5^- ($^1A_1$)	B_5 ($^2B_2$)	2.64	2.47	2.40 ± 0.02
B_6^- ($^2B_{2g}$)	B_6 ($^3B_{3u}$)	3.74	3.12	
B_6^- ($^2B_{2g}$)	B_6 (^1A_g)	3.60	3.17	3.01 ± 0.02
B_7^- ($^1A_1$)	B_7 ($^2B_2$)	2.93	2.87	2.85 ± 0.02
B_7^- ($^3A_2$)	B_7 ($^2B_2$)	2.86	2.92	
B_8^- ($^2B_1$)	B_8 ($^3A_2'$)	3.12	2.99	3.02 ± 0.02
B_8^- ($^2B_1$)	B_8 ($^1A_1'$)	3.56	3.44	3.35 ± 0.02
B_9^- ($^1A_{1g}$)	B_9 ($^2E_{1g}$)	3.63	3.45[b]	3.46 ± 0.02
B_{10}^- ($^2A''$)	B_{10} ($^1A'$)	3.22		3.06 ± 0.03
B_{11}^- ($^1A_1$)	B_{11} ($^2B_2$)	3.63		3.426 ± 0.010
B_{12}^- ($^2A'$)	B_{12} ($^1A'$)	2.41		2.26 ± 0.04
B_{13}^- (^1A_g)	B_{13} ($^2B_{3u}$)	3.98		3.78 ± 0.02

[a] G3B3 calculations of the neutrals using the geometries of the corresponding anions. [b] CCSD(T)/CBS values except for B_9, which was calculated at the CCSD(T)/aVTZ level. [c] Experimental values from ref 25.

TABLE 5: Calculated Singlet−Triplet Gaps (kcal/mol at 0 K) as a Function of the Basis Set at the CCSD(T) Level

reaction	aVDZ	aVTZ	aVQZ	CBS (DTQ)
$B_5^-(\mathbf{II},{}^1A_1) \rightarrow B_5^-(\mathbf{II-t},{}^3B)$	10.5	9.9	9.9	9.9
$B_6(\mathbf{III},{}^1A_1) \rightarrow B_6(\mathbf{IV},{}^3B_u)$	3.3	6.5	7.9	8.8
$B_7^-(\mathbf{IX},{}^1A_1) \rightarrow B_7^-(\mathbf{X},{}^3B_1)$	−0.1	−0.3	−0.3	−0.3
$B_8({}^1A') \rightarrow B_8(\mathbf{XI},{}^3A_2')$	−10.6	−10.5		
$B_9^-(\mathbf{XV},{}^1A_{1g}) \rightarrow B_9^-({}^3A')$	32.9	32.8	32.4	32.0

labeling), which contains 2.8 e for B_5 and 2.7 e for B_5^- located at the center of the five-membered ring. This indicates the presence of a three-center-two-electron (3c-2e) bond in both states, which is likely to be the main factor for stability of these planar structures.

Previous reports in the literature disagreed with each other about the actual number of delocalized π and σ electrons of B_5. Li et al.[56] suggested that there are three and four delocalized π electrons for B_5 and B_5^-, respectively, and that they are aromatic. By using a different approach, Aihara et al.[29] predicted that there are only two delocalized π electrons in each of the two states and that they are both aromatic. From a MO analysis, Zubarev and Boldyrev[6] suggested that in B_5^- there is a conflicting electron distribution with σ-antiaromaticity and π-aromaticity.

The canonical MOs of B_5 and B_5^- reveal that HOMO−3 is a completely bonding orbital containing globally delocalized π electrons, whereas HOMO−1 is a globally bonding σ orbital. These delocalized π and σ orbitals can be considered as the origin for the double aromaticity of B_5 and B_5^-. The SOMO of B_5 (HOMO of B_5^-) is a partially bonding σ orbital with two triangular wings that make an island of σ electron delocalization within the B1−B2−B3 and B3−B4−B5 domains, and thus contributes to the stabilization of the planar structure. The electron populations of the (B1B2), (B1B3), (B2B3B4), (B3B5), and (B4B5) basins in B_5 are close to each other and amount to 2.4, 2.7, 2.8, 2.7, and 2.4 e, respectively. Such a distribution

suggests a homogeneous electron delocalization, and a high degree of aromaticity for B_5. The ELF isosurfaces (Figure 1) also show the existence of two monosynaptic basins at both the B1 and the B5 centers in B_5 and B_5^-, which supports our picture of the bonding. It is clear that the equilibrium structure of either B_5 or B_5^- contains two globally delocalized π electrons, and two globally delocalized σ electrons, each of which satisfies the classical $(4n + 2)$ Hückel rule of aromaticity. In addition, a topological analysis of the ELF_σ component for B_5 and B_5^- was also performed. The bifurcation values of 0.93 for B_5 and 0.91 for B_5^- are high, confirming their σ-aromatic character. Thus, our results suggest that both B_5 and B_5^- clusters have double aromaticity. The ELFs of B_5^+ also given in Figure 1 show that the two monosynaptic basins at the B1 and B5 atoms disappear, so that the cation loses the aromatic character.

B_6. The identity of the most stable B_6 structure has been controversial. Kato et al.,[2] Boustani,[4] Niu et al.,[59] Whiteside,[60] and Li et al.[61] predicted at different levels of theory that the pentagonal pyramid **III** (C_{5v}, $^1A_1$, Figure 1) is the lowest energy form of B_6. However, Ray et al.[3] suggested a square bipyramid ground state at the MP4/3-21G(d) level. More recently, Ma et al.[62] predicted its global minimum structure to be the triplet state **IV-t** (C_{2h}, ^3A_u). Alexandrova et al.[63] and Atis et al.[15] found that both the singlet **III** and the triplet **IV-t** structures (Figure 1) are the lowest-lying isomers from B3LYP and CCSD(T) calculations with 6-311+G(d) and 6-311+G(3df) basis sets.

At the B3LYP/6-31G(d) level, structure **IV-t**, which is a triplet with a valence electron configuration ^3A_u: ...$1a_u^2 3b_u^2$-$4a_g^2 4b_u^1 1b_g^1$, is the lowest-energy state, ~2 kcal/mol below the singlet **III**. In contrast, the higher level calculations show that the singlet pentagonal **III** with a valence electron configuration $^1A_1$: ...$1e_2^4 3a_1^2 2e_1^4$ is lower in energy than the ^3A_u isomer **IV-t**, with a triplet−singlet separation gap of ~6 (G3B3) to ~8 kcal/mol (CCSD(T)/CBS) (see also Table 5). Recent CCSD(T)/6-311+G(2df) calculations[25] also predicted a ground-state singlet with $\Delta E_{ST} = 7.2$ kcal/mol. A high symmetry structure was also located (D_{2h}, ^1A_g), but it is 11 kcal/mol higher than **III** (heat of formation being 290.2 kcal/mol at 0 K, Table 2). The high level calculations thus all predict a singlet ground state **III** ($^1A_1$, C_{5v}) structure with $\Delta E_{ST} \geq 6$ kcal/mol.

For the B_6^- anion as well, the available computational results are not in agreement. Li et al.[61] reported a C_{2v} ($^2A_1$) ground state in which the sixth B atom is capped on the plane on the B3B5 (or B1B3) bond of the B_5 **I** (cf., Figure 1 for atom numbering), rather than a form comparable to the neutral **IV-t**. Subsequent studies[62,63] assigned the low spin, high symmetry D_{2h} **V** structure to be the most stable isomer with a valence electron configuration of $^2B_{2g}$: ...$1b_{3g}^2 1b_{3u}^2 3a_g^2 2b_{2u}^2 2b_{1u}^2 1b_{2g}^1$. An interesting feature of the $^2B_{2g}$ structure is that it resembles a dimer of B_3 in which the interaction of the two BB bonds gives rise to a rectangular subunit. A structure having a ^2B_u (C_{2h}) state is reported to be 6.2 kcal/mol higher in energy than **V** at the UB3LYP/6-311+G(d) level.[63]

Our calculations show that there are a substantial number of low energy states/structures for B_6^-. We first located structures **V** and **VI**, which have a similar shape. Structure **V** (D_{2h}, $^2B_{2g}$) is the one previously identified. At the UMP2/aVDZ level, there is substantial spin contamination, and there are two large imaginary frequencies consistent with symmetry breaking in the wave function. Structure **VI** (C_{2h}, ^2B_u) is a first-order saddle point with a small imaginary frequency (244i cm^{-1}) at the UB3LYP level, whereas the UMP2 calculations show it as an equilibrium structure having all real vibrational frequencies. Again, there is substantial spin contamination in the UHF wave function. Three other structures were also identified (Table 1). Structure **V-u** is in the D_{2h} point group similar to **V** but has a $^2B_{1u}$ electronic state. Structure **V-c**, which is basically derived from an in-plane deformation of **V**, is in the C_{2h} point group with a ^2A_u electronic state. Structure **V-s** arises from electron attachment to the neutral **III**, which first leads to a vertical anion in a $^2E_1$ state and then undergoes a Jahn−Teller distortion to form structure **V-s**. The TAE(CBS) values obtained for the five different states of B_6^- are given in Table 1, and their heats of formation are shown in Table 2.

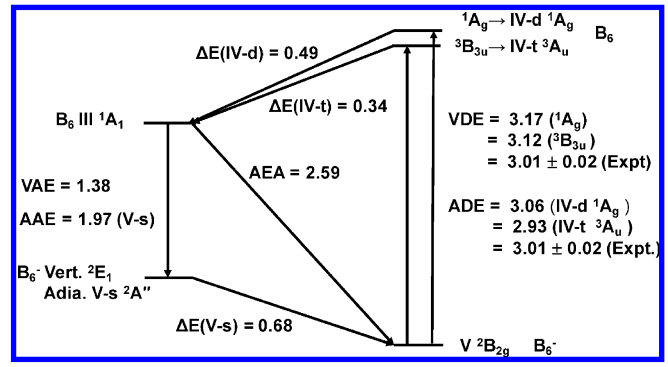

Figure 3. Calculated energies in eV for the different transitions in the B_6/B_6^- system.

At the CCSD(T)/CBS level, using the MP2 geometries, **V** ($^2B_{2g}$) is only 1 kcal/mol lower in energy than **VI** (^2B_u). Because of the closeness in the energies of these two structures, we reoptimized both geometries at the R-UCCSD(T)/aVDZ level. The CCSD(T)/CBS energies based on the CCSD(T) geometries persist showing that **V** ($^2B_{2g}$) is 6.5 kcal/mol lower in energy than **VI** (^2B_u) (cf., Tables 1 and 2). The structures **V-u** ($^2B_{1u}$), **V-c** (^2A_u), and **V-s** ($^2A''$) are calculated to be 15.5, 24.9, and 15.7 kcal/mol above **V**, respectively.

The G3B3 heat of formation of 213.0 kcal/mol for **V** differs substantially from the CBS value of 220.8 kcal/mol, probably due to the spin contamination problems inherent in using a UHF wave function. The deviations of the G3B3 values with respect to the CCSD(T)/CBS counterparts are indeed substantial. The global adiabatic EA(B_6) evaluated as the difference between the heats of formation at 0 K of B_6 **III** (C_{5v}, $^1A_1$) and B_6^- **V**(D_{2h}, $^2B_{2g}$) is 2.53 eV at the CBS level. The G3B3 value of 3.23 eV is too large due to issues with using the UHF wave function. The experimental value is 3.01 ± 0.04 eV.[63] The difference between the calculated adiabatic EA and experimental ADE is due to the fact that the experimental ADE yields a B_6 structure like **V** with approximate D_{2h} symmetry.

To provide a better comparison between the calculated and experimental values, we calculated the VDE of **V** using the CCSD(T)/CBS method. To illustrate the complex situation concerning the B_6/B_6^- system, Figure 3 summarizes the calculated energies for the different structures. Removal of one electron from B_6^- **V** leads to a neutral species having either a singlet or a triplet state. The resulting vertical singlet (^1A_g) and triplet ($^3B_{3u}$) states are close in energy, 3.17 and 3.12 eV, respectively, above **V**. Again, the corresponding G3B3 values are much larger than the CCSD(T)/CBS results (Table 4). The two CBS values are consistent with the experimental VDE of 3.01 eV.[63]

Starting with the vertical ^1A_g state, a stationary point **IV-d** with D_{2h} symmetry was located with one imaginary frequency. The imaginary vibrational mode b_{3u} of 69i cm^{-1} (B3LYP/aVTZ) corresponds to an out-of-plane cis-bent distortion. Upon geometry relaxation along this mode, a C_2 equilibrium structure **IV-s**

TABLE 6: Binding Energies (D_e) and Average Binding Energies (E_b) of the B_n and B_n^- Clusters (eV)[a]

n	E_b (B_n)[b]	E_b (B_n^-)[c]	D_e (B_n)[d]	D_e (B_n^-)[e]
2	1.42	2.41	2.79	4.56
3	2.82	3.80	5.68	6.57
4	3.40	3.82	5.23	3.89
5	3.65	4.14	4.68	5.44
6	3.80	4.33	4.58	5.29
7	4.08	4.47	5.82	5.30
8	4.31	4.70	5.83	6.30
9	4.36	4.69	4.71	4.62
10	4.50	4.79	5.82	5.64
11	4.54	4.86	4.97	5.60
12	4.65	4.85	5.85	3.92
13	4.63	4.91	4.30	6.37

[a] Values obtained from the G3B3 heats of formation at 0 K. [b] Using eq 5a. [c] Using eq 5b. [d] Using eq 4a. [e] Using eq 4b.

(C_2, ^{1}A) is located, but the energy difference between both D_{2h} and C_2 structures is small (0.4 kcal/mol, Table 1). After including all of the corrections shown in Table 1, **IV-d** becomes 0.4 kcal/mol lower in energy than **IV-s**. This energy difference increases to 1.0 kcal/mol at 298 K in favor of **IV-d** (Table 2). In view of the flat potential energy surface, we can conclude that the singlet neutral structure formed following electron detachment from B_6^- **V** essentially conserves the D_{2h} point group. The adiabatic energy separation between **IV-d** and **V** is 3.06 eV (Figure 3) in agreement with experiment.

Geometry optimization starting from the vertical $^3B_{3u}$ point leads to a D_{2h} stationary point with one imaginary frequency. Relaxation of the geometry along the imaginary vibrational mode of this structure (b_{3g} mode of 143i cm^{-1} at B3LYP/aVDZ) yields the equilibrium structure **IV-t** (C_{2h}, ^3A_u) described above. The energy gain upon relaxation is 7.1 kcal/mol, and this triplet state is lower than the D_{2h} state for B_6, although neither is the global minimum. The **IV-t** − **V** energy difference is 2.93 eV, again in agreement with the experimental ADE. Because of the similarity between their vertical D_{2h} and equilibrium D_{2h}/C_{2h} structures, both transitions of $B_6 \leftarrow B_6^-$ giving the singlet and triplet neutral could be observed by the PES experiment, and the CBS ADE values of 3.06 eV (**IV-d** ← **V**) and 2.93 eV (**IV-t** ← **V**) are in excellent agreement with the experimental estimate of 3.01 ± 0.02 eV.[63]

Li et al.[61] derived an AEA(B_6) of ~2.0 eV from DFT (B3LYP and B3PW91) calculations of **V** for B_6 and a $^2A_1$(C_{2v}) state for B_6^-. Using B3LYP/6-311+G(3df) calculations, Ma et al.[62] reported a value of 2.60 eV for this quantity considering **IV-t** for B_6 and **V** for B_6^- as the lowest-energy structures. The latter B3LYP value can be compared to the ADE of 2.53 eV (CCSD(T)/CBS) given above. The difference is mainly due to the different assignments of the ground state.

Although there is now a consensus on the global minimum structure of B_6, the appropriate description of its chemical bonding remains a matter of debate. On the basis of the NICS indices, Ma et al.[62] predicted that both B_6 and B_6^- are nonaromatic. By using current density maps, Alexandrova et al.[63] stated that B_6^- **V** ($^2B_{2g}$) is doubly antiaromatic. Aihara et al.[29] argued that the B_6 clusters are aromatic in the neutral, anion, and dianion states. More recently, Zubarev and Bolderev[6] considered that B_6 in its planar configuration ($^1A_1'$, D_{5h}) is doubly aromatic. The dianion B_6^{2-} ($^2B_{2g}$, D_{2h}) planar configuration is also predicted to be doubly antiaromatic, but exhibits some islands for σ and π aromaticity.

Our MO and ELF analyses support the view that neutral B_6 is doubly aromatic, and that B_6^- is partially aromatic. From

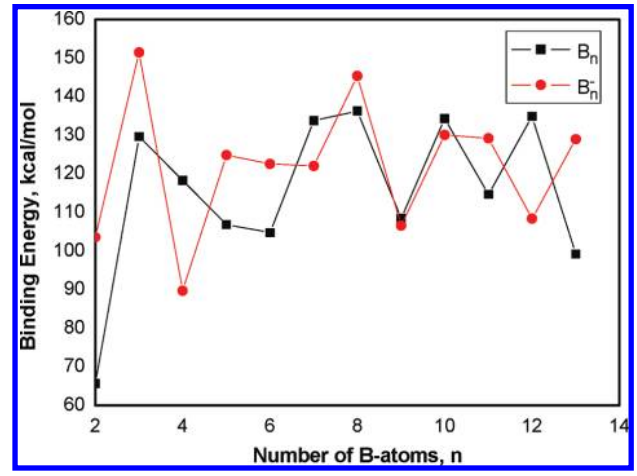

Figure 4. Size dependence of the binding energies (D_e in kcal/mol) of B_n and B_n^- clusters. Values obtained from G3B3 heats of formation at 0 K.

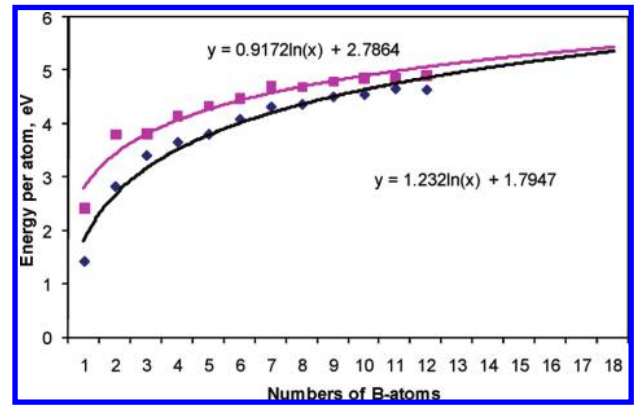

Figure 5. Size dependence of the average energy per atom (E_b in eV) of B_n (black line) and B_n^- (violet line) clusters. Values obtained from G3B3 heats of formation at 0 K.

the total ELF map for B_6 **III** in Figure 1, the five basins (B1B2B6), (B1B5B6), (B2B4B6), (B3B5B6), and (B3B4B6) are characterized as trisynaptic with each containing ~3.5 e. This shows the existence of 3c-2e bonds between two boron atoms in the five-membered ring to the central boron. These populations are equally partitioned into σ and π electrons and delocalized over the whole structure. To simplify the interpretation, we now consider a higher symmetry structure (D_{5h}, $^1A_1'$) for the neutral cluster in which the central atom is pushed into the center in the molecular plane. The MO diagrams for the neutral D_{5h} form show that there are six bonding σ electrons and two bonding π electrons distributed among the three bonding σ orbitals (the degenerate HOMO and HOMO−1), and one bonding π orbital (HOMO−3), respectively. The number of σ (6) and π (2) electrons formally satisfy the conventional Hückel rule of aromaticity, and such an electron partition makes B_6 (D_{5h}, $^1A_1'$) doubly aromatic. This result can be applied to the global minimum structure **III** (C_{5v}). The ELF$_\sigma$ of B_6 (C_{5v}) is plotted separately to identify the values of bifurcations. The high value of 0.89 for ELF$_\sigma$ suggests that **III** also has σ aromatic character, and the neutral B_6 is a doubly σ and π aromatic system.

To simplify the analysis for the open shell B_6^- anion, we first consider the closed shell B_6^{2-} dianion. From the MO diagrams of the global minimum B_6^{2-} (D_{2h}) with a valence orbital configuration of $^1A_{1g}$: $1a_g^2 1b_{1u}^2 2a_g^2 1b_{2u}^2 1b_{3g}^2 3a_g^2 2b_{2u}^2 2b_{1u}^2 1b_{2g}^2$, the dianion can easily be identified with two global bonding orbitals (HOMO for π and HOMO−3 for σ) and two

partially bonding orbitals (HOMO−4 for π and HOMO−1 for σ). The HOMO and HOMO−3 exhibit bonding electron delocalization over the entire cluster, leading to global (σ and π) aromaticity, whereas the remaining electrons form islands. The total ELF reveals that six disynaptic basins are formed from six B ring atoms, in which each of the two (B1B2) and (B3B4) basins contains ∼2.5e, and each of the remaining basins contains ∼3.4e (see Figure 1 for atom numbering). Such a distribution exhibits a high electron concentration within each of the two three-membered (B_3^-) components and thus supports further the viewpoint of the partial electron delocalization of the dianion. When analyzing the ELF_σ and ELF_π separately, a very high bifurcation value of 0.91 for ELF_σ is found. This is even higher than the bifurcation value of 0.79 found for Al_4^{2-} that was demonstrated to be a multiply aromatic system.[48,51] Thus, we can assign B_6^{2-} as a σ aromatic system. For the ELF_π component, there are two distinct regions; although the first bifurcation value of 0.6 for the separation of two reducible basins is low, the second value is very high. In addition, the basins cannot be separated further; even the ELF_π isosurface attains a high value of 0.99. This observation is consistent with the view that the B_6^{2-} is globally non π aromatic, but contains islands of π aromaticity.

For the B_6^- radical anion, which is formed upon removal of an electron from the dianion, the unpaired electron is of π character in the $^2B_{2g}$ **V**, and, as a consequence, the global character of the bonding in the cluster is not changed.

B_7. Our calculations predict that the neutral B_7 ground state exhibits a nearly planar hexagon capped by one element at the center **VII** (C_{2v}, Figure 1) with a valence orbital configuration of $^2B_2$: $1a_1^2 1b_2^2 1b_1^2 2a_1^2 1a_2^2 3a_1^2 2b_1^2 4a_1^2 2b_2^2 3b_1^2 3b_2^1$, which agrees well with previous theoretical results.[2,8,15,24,64,65] The other C_{2v} alternative **VIII** ($^2B_2$) structure is predicted to be ∼27 kcal/mol higher in energy.

The lowest-lying structure of B_7^- is not as well established. From B3LYP, B3PW91, and MP2 calculations, Li et al.[65] predicted that the anion cluster has a singlet ground state **IX** (C_{2v}, $^1A_1$: $1a_1^2 1b_2^2 1b_1^2 2a_1^2 1a_2^2 3a_1^2 2b_1^2 4a_1^2 2b_2^2 3b_1^2 3b_2^2$). On the contrary, Alexandrova et al.[64] reported that B_7^- has the high spin pyramidal **X** ($^3A_1$, C_{6v}) as its most stable isomer. However, at the RCCSD(T)/6-311+G(2df) level, the triplet **X** structure is only 0.7 kcal/mol lower in energy than the singlet **IX**. G3B3 calculations predict that the energy difference between both states is small and that the low spin state is favored by 1.1 kcal/mol. Similarly, the CCSD(T) calculations predict a singlet−triplet separation gap of 0.3 kcal/mol at the CBS limit, but in an opposite direction in favor of the high spin state (Table 5), and it is only upon inclusion of the additional corrections that the lower spin state becomes more stable by 1.3 kcal/mol (Table 2). We thus conclude that B_7^- has the low symmetry, low spin ground state **X** (C_{2v}, $^1A_1$) but that there is a very close lying $^3A_1$, C_{6v} state.

The VDE derived from **X** ($^3A_1$) is calculated to be 2.86 and 2.92 eV at the G3B3 and CCSD(T) levels, respectively, and the respective G3B3 and CCSD(T) VDEs from B_7^- **IX** are 2.93 and 2.87 eV. Both are in excellent agreement with the experimental value of 2.85 eV.[64] The G3B3 and CBS adiabatic electron affinities EA(B_7) are 2.72 and 2.62 eV, respectively (Table 3), and both compare favorably with the experimental value of 2.55 ± 0.05 eV.[64]

We found that the planar high symmetry triplet (D_{6h}, $^3A_{1g}$: $1a_{1g}^2 1e_{1u}^4 1e_{2g}^4 1a_{2u}^2 2a_{1g}^2 1b_{2u}^2 2e_{1u}^4 1e_{1g}^2$) is, although not a local minimum, a low-energy form being only ∼1 kcal/mol higher in energy than **IX** at the G3B3 level. The UB3LYP/6-31G(d) geometry of this $^3A_{1g}$ state is characterized by all equal BB distances of 1.626 Å, including those connecting the central atom to the peripheral atoms. The lower symmetry forms **IX** and **X** can be considered as small distortions from the D_{6h} ($^3A_{1g}$) structure. The MOs of these different structures of B_7^- have been shown to be similar.[64] To simplify the discussion, we only describe the ELFs of the D_{6h} structure.

The topology of the ELF supports the view that the planar B_7^- anion cluster is a π aromatic system. The ELF plots show bifurcation values of ELF_σ and ELF_π of 0.92 and 0.91, respectively, making planar B_7^- a doubly aromatic molecule. For the singlet B_7^- **IX**, the bifurcation value of 0.94 for ELF_σ suggests σ aromaticity. The value of 0.81 for its ELF_π is rather low with respect to the corresponding value of 0.91 for benzene, so it suggests a weak π-aromaticity. The total ELF plots emphasize the existence of four disynaptic basins (B1B2), (B1B6), (B3B4), and (B3B5) between the peripheral atoms, in which each basin contains ∼2.6 e. Each of the two trisynaptic basins (B2B7B5) and (B4B7B6) contains ∼4.4 e, which again indicates the presence of three-center bonds in the singlet state **IX** (C_{2v}, $^1A_1$). These three-center bonds and σ aromatic character are consistent with a high stability for the $^1A_1$ state, irrespective of the fact that the system is only weakly π-aromatic.

B_8. Kato et al.[2] predicted a singlet structure (C_{2v}, $^1A_1$) for the neutral B_8 cluster, whereas Ray et al.[3] predicted a square antiprism form. Reis et al.[66] reported a high symmetry high spin geometry (D_{7h}, $^3B_2'$) structure. Many subsequent theoretical studies[16,67−70] using various levels of theory predicted a different ground state. Our calculations concur with the view that the most stable B_8 structure features a heptagon **XI** (D_{7h}), but with a high spin $^3A'_2$ ground state. The alternative low spin C_{2v} ($^1A_1$) structure that results from a Jahn−Teller distortion of the unstable D_{7h} singlet state is 8.6 kcal/mol higher in energy than **XI**.

For the B_8^- radical anion, the planar arrangement **XII** (C_{2v}, $^2B_1$) arising from a slight in-plane distortion of the heptagonal neutral B_8 is predicted to be the most stable isomer.[70] Because the B_8^- anion has a doublet ground state, detachment of one electron from it can lead to either a singlet or a triplet neutral. The VDE evaluated from structure **XII** ($^2B_1$) is 3.12 (G3B3) and 2.99 (CCSD(T)/CBS) eV to form a vertical triplet neutral ($^3A_2'$), and 3.56 (G3B3) and 3.44 (CCSD(T)/CBS) eV to produce a vertical singlet neutral ($^1A_1'$) (Table 4). The CCSD(T)/CBS values are in excellent agreement with the experimental VDE values of 3.02 ± 0.02 and 3.35 ± 0.02 eV.[70] An adiabatic EA of 3.11 and 3.02 eV is predicted at the G3B3 and CCSD(T) levels between the $^3A'_2$ state of B_8 and the $^2B_1$ state of B_8^-. For this system, the experimental adiabatic EA(B_8) was assigned to be the same as the VDE(B_8^-).[70] The fact that there is only a very small difference (0.01 eV) between the calculated ADE and VDE of B_8^- is consistent with the seven-member rings characterizing both states changing only slightly on electron addition.

In the MO wave function of B_8, there are four π electrons distributed over three global bonding π orbitals (HOMO(e) and HOMO−2) and six σ electrons over three bonding σ orbitals (HOMO−1(e) and HOMO−4). The topological features of the total ELF shown in Figure 1 are associated with the high bifurcation values of 0.94 and 0.91 for the ELF_π and ELF_σ components, respectively, and show the doubly σ and π aromaticity of B_8.

B_9. The identity of the most stable structure of the neutral nine boron cluster has not been well established yet.[70] Boustani[4] predicted two lower-lying isomers including a nonplanar C_s and

TABLE 7: Reaction Energies (ΔH_r) of Dissociative Processes Forming B_3 and B_4 Rings, Evaluated from G3B3 Heats of Formation (0 K, kcal/mol)

dissociation reaction of B_n and B_n^-	$-\Delta H_r$	dissociation reaction of B_n and B_n^-	$-\Delta H_r$
$B_3(^2A_1') \rightarrow B_2(^3\Sigma_g^-) + B(^2P)$	129.7	$B_9^-(^1A_{1g}) \rightarrow B_2^-(^4\Sigma_g^-) + B_7(^2B_2)$	203.6
$B_3(^1A_1') \rightarrow B_2^-(^4\Sigma_g^-) + B(^2P)$	151.5	$B_9^-(^1A_{1g}) \rightarrow B_3^-(^1A_1') + B_6(^1A_1)$	185.9
$B_4(^1A_g) \rightarrow 2B_2(^3\Sigma_g^-)$	182.3	$B_9^-(^1A_{1g}) \rightarrow B_4^-(^2B_{1u}) + B_5(^2B_2)$	201.1
$B_4(^1A_g) \rightarrow B_3(^2A_1') + B(^2P)$	118.3	$B_{10}(^1A_g) \rightarrow B_2(^3\Sigma_g^-) + B_8(^3A_2')$	177.1
$B_4^-(^2B_{1u}) \rightarrow B_2^-(^4\Sigma_g^-) + B_2(^3\Sigma_g^-)$	175.4	$B_{10}(^1A_g) \rightarrow B_3(^2A_1') + B_7(^2B_2)$	183.7
$B_4^-(^2B_{1u}) \rightarrow B_3^-(^1A_1') + B(^2P)$	89.6	$B_{10}(^1A_g) \rightarrow B_4(^1A_g) + B_6(^1A_1)$	199.2
$B_5(^2B_2) \rightarrow B_2(^3\Sigma_g^-) + B_3(^2A_1')$	159.5	$B_{10}^-(^2A') \rightarrow B_2^-(^4\Sigma_g^-) + B_8(^3A_2')$	197.4
$B_5(^2B_2) \rightarrow B_4(^1A_g) + B(^2P)$	106.9	$B_{10}^-(^2A'') \rightarrow B_3^-(^1A_1') + B_7(^2B_2)$	182.2
$B_5^-(^1A_1) \rightarrow B_2^-(^4\Sigma_g^-) + B_3(^2A_1')$	171.2	$B_{10}^-(^2A'') \rightarrow B_4^-(^2B_{1u}) + B_6(^1A_1)$	226.4
$B_5^-(^1A_1) \rightarrow B_4^-(^2B_{1u}) + B(^2P)$	125.5	$B_{11}(^2B_2) \rightarrow B_2(^3\Sigma_g^-) + B_9(^2B_{1g})$	183.3
$B_6(^1A_1) \rightarrow B_2(^3\Sigma_g^-) + B_4(^1A_g)$	146.0	$B_{11}(^2B_2) \rightarrow B_3(^2A_1') + B_8(^3A_2')$	162.1
$B_6(^1A_1) \rightarrow 2B_3(^2A_1')$	134.6	$B_{11}(^2B_2) \rightarrow B_4(^1A_g) + B_7(^2B_2)$	180.1
$B_6^-(^2B_{2g}) \rightarrow B_2^-(^4\Sigma_g^-) + B_4(^1A_g)$	175.0	$B_{11}^-(^1A_1) \rightarrow B_2^-(4\Sigma_g^-) + B_9(^2B_{1g})$	218.1
$B_6^-(^2B_{2g}) \rightarrow B_3^-(^1A_1') + B_3(^2A_1')$	141.8	$B_{11}^-(^1A_1) \rightarrow B_3^-(^1A_1') + B_8(^3A_2')$	175.1
$B_7(^2B_2) \rightarrow B_2(^3\Sigma_g^-) + B_5(^2B_2)$	172.9	$B_{11}^-(^1A_1) \rightarrow B_4^-(^2B_{1u}) + B_7(^2B_2)$	221.8
$B_7(^2B_2) \rightarrow B_3(^2A_1') + B_4(^1A_g)$	150.1	$B_{12}(^1A_1) \rightarrow B_2(^3\Sigma_g^-) + B_{10}(^1A_g)$	183.9
$B_7^-(^1A_1) \rightarrow B_2^-(^4\Sigma_g^-) + B_5(^2B_2)$	190.2	$B_{12}(^1A_1) \rightarrow B_3(^2A_1') + B_9(^2B_{1g})$	188.5
$B_7^-(^1A_1) \rightarrow B_3^-(^1A_1') + B_4(^1A_g)$	145.6	$B_{12}(^1A_1) \rightarrow B_4(^1A_g) + B_8(^3A_2')$	178.7
$B_8(^3A_2') \rightarrow B_2(^3\Sigma_g^-) + B_6(^1A_1)$	204.4	$B_{12}^-(^2A') \rightarrow B_2^-(^4\Sigma_g^-) + B_{10}(^1A_g)$	192.2
$B_8(^3A_2') \rightarrow B_3(^2A_1') + B_5(^2B_2)$	179.5	$B_{12}^-(^2A') \rightarrow B_3^-(^1A_1') + B_9(^2B_{1g})$	175.0
$B_8(^3A_2') \rightarrow 2B_4(^1A_g)$	168.1	$B_{12}^-(^2A') \rightarrow B_4^-(^2B_{1u}) + B_8(^3A_2')$	193.9
$B_8^-(^2B_1) \rightarrow B_2^-(^4\Sigma_g^-) + B_6(^1A_1)$	230.8	$B_{13}(^2A_2) \rightarrow B_2(^3\Sigma_g^-) + B_{11}(^2B_2)$	168.4
$B_8^-(^2B_1) \rightarrow B_3^-(^1A_1') + B_5(^2B_2)$	184.1	$B_{13}(^2A_2) \rightarrow B_3(^2A_1') + B_{10}(^1A_g)$	153.4
$B_8^-(^2B_1) \rightarrow B_4^-(^2B_{1u}) + B^4(^1A_g)$	201.4	$B_{13}(^2A_2) \rightarrow B_4(^1A_g) + B_9(^2B_{1g})$	169.4
$B_9(^2A_1) \rightarrow B_2(^3\Sigma_g^-) + B_7(^2B_2)$	179.1	$B_{13}^-(^1A_g) \rightarrow B_2^-(^4\Sigma_g^-) + B_{11}(^2B_2)$	206.5
$B_9(^2A_1) \rightarrow B_3(^2A_1') + B_6(^1A_1)$	183.2	$B_{13}^-(^1A_g) \rightarrow B_3^-(^1A_1') + B_{10}(^1A_g)$	169.7
$B_9(^2A_1) \rightarrow B_4(^1A_g) + B_5(^2B_2)$	169.7	$B_{13}^-(^1A_g) \rightarrow B_4^-(^2B_{1u}) + B_9(^2B_{1g})$	214.4

a heptagonal bipyramid D_{7h} structure constructed from a flat hexagonal pyramid. Zhai et al.[16] predicted that the high symmetry, low spin wheel-like structure **XIV** (D_{2h}, $^2B_{1g}$) possesses the lowest energy (Figure 2). At the B3LYP/6-311+G(d) level, the second lowest-lying isomer (3.2 kcal/mol higher in energy) is a slightly distorted heptagonal bipyramid

TABLE 8: Calculated Resonance Energies (RE) and Normalized Resonance Energies (NRE) of the B_n and B_n^- Clusters ($n = 5-13$) as a Function of the Number of BB Bonds (m)[a]

cluster B_n	number of BB bonds	RE (B_n)[b]	RE (B_n^-)[c]	NRE (B_n)	NRE (B_n^-)
3	3	44.2	50.7	14.7	16.9
4	5	61.7	39.6	15.4	9.9
5	7	67.8	64.2	13.6	12.8
6	9	71.8	85.5	11.9	14.3
	10	21.4	35.1	3.6	5.9
7	11	104.8	106.8	15.0	15.3
	12	54.4	56.4	7.8	8.1
8	13	140.3	151.4	17.5	18.9
	14	89.9	101.0	11.2	12.6
9	15	148.0	157.2	16.4	17.5
	16	97.6	106.8	10.8	11.9
10	17	181.5	186.5	18.2	18.7
	18	131.1	136.1	13.1	13.6
11	19	195.4	214.9	17.8	19.5
	20	145.0	164.5	13.2	15.0
	21	94.6	114.1	8.6	10.4
12	21	229.5	222.5	19.1	18.6
	22	179.1	172.1	14.9	14.3
	24	78.3	71.3	6.5	5.9
13	23	227.9	250.7	17.5	19.3
	24	177.5	200.3	13.7	15.4
	26	76.7	101.5	5.9	7.8

[a] Values given in kcal/mol. [b] Using eq 6a with the TAE(B_2 ($^1\Sigma_g^+$)) = 50.4 kcal/mol. [c] Using eq 6b with the TAE(B_2^- ($^4\Sigma_g^-$)) = 111.1 kcal/mol.

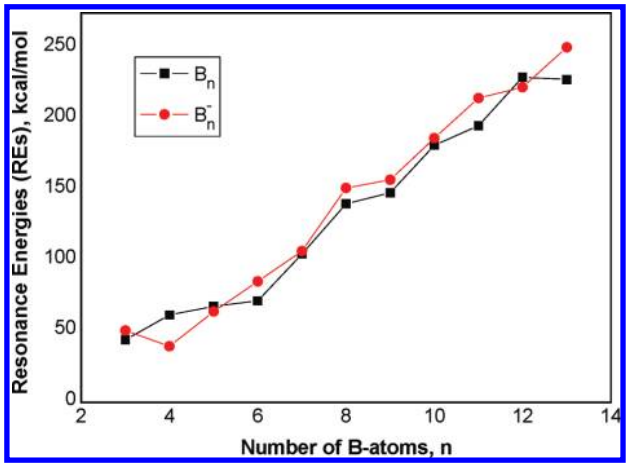

Figure 6. Size dependence of the resonance energies (RE in kcal/mol) of B_n and B_n^- clusters. Values obtained from G3B3 heats of formation at 0 K.

XIII (C_{2v}, $^2A_1$). Kato et al.[2] predicted earlier that **XIII** is the global minimum isomer. Our G3B3 results predict that in the low spin manifold, the low symmetry Jahn−Teller distorted structure **XIII** corresponds to the most stable isomer, which is 11.3 kcal/mol lower in energy than the higher symmetry **XIV**.

For the anion B_9^-, we find the high symmetry planar structure **XV** (D_{8h}, $^1A_{1g}$) to be the global minimum, in agreement with a previous prediction.[16] The next highest energy isomer is a heptagonal bipyramid structure (D_{7h}, $^1A_1$), which is 10.6 kcal/mol higher in energy. In both neutral and anionic forms, the high spin states are much less stable and were not further considered.

The VDE of the anion **XV** is generated by removing one electron from its HOMO producing a vertical $^2E_{1g}$ state. The G3B3 and CCSD(T)/aVTZ values of 3.63 and 3.45 eV respectively are consistent with the PES result of 3.46 ± 0.02 eV.[70] The global adiabatic EA can be defined as the energy difference between ground-state anion XV and ground-state neutral XIII and is 3.03 eV. The experimental ADE is 3.39 ± 0.06 eV[15] in excellent agreement with our G3B3 value of 3.53 eV for the energy difference between **XV** and **XIV**, which have the same molecular shape.

Similar to the electronic configuration of B_8, the MO picture of B_9^- shows three bonding π orbitals (HOMO(e) and HOMO−2) and three σ bonding orbitals (HOMO−1(e) and HOMO−4). Thus, six π electrons and six σ electrons are distributed within the high symmetrical skeleton of B_9^- **XV**, consistent with its aromaticity based on the ELF analysis below.

The ELF maps for B_9 (D_{7h}, $^2A_1$) and B_9^- (D_{8h}, $^1A_{1g}$) show the presence of seven distinct disynaptic basins between the peripheral atoms of the heptagonal bipyramid (D_{7h}, $^2A_1$), in which each basin contains ~2.7e. This perfect electron delocalization in the high symmetry form (D_{7h}, $^2A_1$) is consistent with high structural stability. For the planar anion (D_{8h}, $^1A_{1g}$), a similar landscape emerges. Each of the eight peripheral disynaptic basins contains ~3.0e. This more complete electron delocalization inherently stabilizes the structure. The bifurcation value of 0.97 for ELF_π is very high and clearly indicates a strong π aromaticity. The value of ELF_σ of 0.87 is higher than that of benzene. These results show that B_9^- **XV** possesses double aromaticity consistent with the MO picture.

B_{10}. There is consensus as to the global minimum structures of both B_{10} and B_{10}^- (Figure 2). Apart from the prediction made by Boustani[4] that B_{10} has the convex C_{2v} structure, its global minimum has been established to be a nearly planar C_{2h} structure **XVI** (^1A_g).[2,16,71] The most stable structure for B_{10}^- is the planar C_s form **XVII** ($^2A''$).[16] Our calculations concur with these findings. We also considered for B_{10} two additional high symmetry geometries, a perfect plane (D_{9h}, $^1A_1'$) and an octagonal bipyramid (D_{8h}, $^1A_{1g}$) structure. These were however found to be much higher in energy than the global minimum.

The VDE evaluated by detaching one electron from the HOMO of the C_{2h} (^1A_g) structure is 3.22 eV at the G3B3 level, in reasonable agreement with the experimental result of 3.06 ± 0.03 eV,[26] and consistent with the differences found for the other B_n clusters. The adiabatic EA of 2.85 eV obtained from the relevant G3B3 heats of formation is consistent with the experimental value of 2.88 ± 0.09 eV.[26]

Again, the shape of MOs and the topology of ELF were constructed for a higher symmetry structure of B_{10}, D_{2h} (^1A_g), in which two out-of-plane inner atoms are placed in the ring plane. There are three bonding π orbitals (HOMO, HOMO−1, and HOMO−4) and three bonding σ orbitals (HOMO−2, HOMO−3, and HOMO−4), which contain six π and six σ electrons, respectively, and thus satisfy the Hückel rule. The bifurcation value of ELF_π is 0.76, close to the value of 0.78 previously obtained for naphthalene by Santos et al.[51] The ELF_π values for the polycyclic species are smaller than that of benzene (0.91). The value of ELF_σ is very high, 0.95. Although distortion from this ideal D_{2h} structure yielding the minimum C_{2h} is expected to reduce the electron delocalization, a doubly (σ and π) aromatic character can be assigned to the neutral cluster B_{10}.

B_{11}. Kato et al.[2] reported a C_{2v} ($^2A_1$) structure to be the most stable structure for B_{11}, whereas Boustani[4] reported a quasi-planar C_s ($^2A''$) structure containing a shallow hexagonal unit connected to a heptagonal pyramid. Zhai et al.[16] found a similarly shaped structure but with C_{2v} symmetry and a $^2B_2$ state (**XVIII**, Figure 2). According to our calculations, there is only marginal difference in energy (~0.3 kcal/mol) between a C_s

and a C_{2v} structure of the type **XVIII**, which both exist on a flat potential energy surface. We conclude that the C_{2v} structure **XVIII** ($^2B_2$) is the ground state of B_{11}. The alternative structure **XIX** is ~10 kcal/mol higher in energy.

Similar structures are obtained for the anionic cluster B_{11}^-. However, for the anion, both C_{2v} structures **XX** and **XXI** have the same energy with the former being only 0.3 kcal/mol lower at 0 K, but 0.1 kcal/mol higher at 298 K than the latter.

The adiabatic EA and anion VDE calculated by detaching one electron from the HOMO of B_{11}^- **XX** (C_{2v}, $^2B_2$) at the G3B3 level are 3.48 and 3.63 eV, respectively. The VDE agrees reasonably well with the PES result of 3.426 ± 0.010 eV.[70] The experimental work[70] suggested that the EA and VDE quantities are identical.

The three bonding π orbitals (HOMO, HOMO−2, and HOMO−6) and four bonding σ orbitals (HOMO−1, HOMO−3, HOMO−4, and HOMO−5) in B_{11} are responsible for its σ antiaromatic and π aromaticity, respectively.[6] These authors postulated that the globally delocalized electrons can break into four different areas leading to σ aromatic islands. Our ELF analysis reveals that the first bifurcation value of ELF_σ of 0.80 is for isosurfaces separated into four isolated basins, whereas the second value of 0.91 is for separating it completely. The ELF_π value of 0.98 is high and shows that B_{11}^- has global π aromaticity.

B_{12}. The geometry and electronic structure of B_{12} and its anion were extensively investigated by different authors.[2,4,15,16,29,72,73] Our G3B3 calculations confirm previous prediction that the structure **XXII** (C_{3v}, ^1A_g), consisting of three hexagonal pyramids as subunits, constitutes the most stable isomer. The cluster is slightly distorted out-of-the-plane but is rather fluxional as the fully planar D_{3h} structure lies only 3.7 kcal/mol higher in energy.

Following attachment of one electron to the doubly degenerate LUMO of B_{12}, the C_{3v} structure undergoes a Jahn−Teller distortion, giving rise to a three-dimensional C_s structure **XXIII** ($^2A'$) for the anion B_{12}^- (Figure 2). G3B3 calculations yield the values of 2.33 and 2.41 eV for EA(B_{12}) and VDE(B_{12}^-), respectively, in good agreement with the PES results of 2.21 ± 0.04 and 2.26 ± 0.04 eV.[26]

Earlier theoretical studies have focused on π-electron delocalization as an important component for B_{12} where six π-electrons occupy orbitals similar to that of benzene. However, as discussed above, B_{10} and B_{11}^- also have benzene-like 6 π-electrons, but their HOMO−LUMO gaps are found to be much smaller than that of B_{12}. Thus, simple π-electrons cannot account for the differences. Zubarev and Boldyrev[6] argued that the three central B atoms donate electrons to form islands of σ-electrons where each pair of delocalized electrons is affiliated with three or four B atoms.

As described in previous studies,[2,4,15,16,29,74,75] the BB bond distances in the B_9 subunit of B_{12} (1.55−1.61 Å) are similar to that of B_2 (1.59 Å), and all are shorter than those in the B_3 subunit (1.65 Å). The inter-ring B−B distances formed between the atoms 2, 5, and 7 of the inner B_3 subset with the atoms of the outer B_9 ring (cf., structure XXII in Figure 2 for atom numbering) are longer, 1.68−1.81 Å. The distances suggest that in structure **XXII** there are 24 BB interactions that could be considered as some type of bond formed by the 36 valence electrons of B_{12}. These 36 electrons are distributed as follows: (i) 18 σ-electrons are used to make the nine BB bonds of the outer B_9 cycle; (ii) 6 σ-electrons to make the three bonds of the inner B_3 cycle; (iii) 6 π-electrons are delocalized over the entire cluster; and (iv) the remaining 6 electrons are delocalized between the B_9 and B_3 rings. Thus, beside the B_9 skeleton, there is a $6_\sigma-6_\pi-6_{\sigma delo}$ trifurcation of electrons. Aihara et al.[29] predicted that the π-delocalization in planar boron clusters reaches a maximum point at B_{12}. An important result from this analysis is that, in addition to the π-electrons, there are MOs between B_9 and B_3 subunits that contribute to a stabilization of the B_{12} cluster. All of the subsets can formally be considered as aromatic $(4n + 2)$ units.

The above description based on orbital interactions can also be obtained from a topological analysis of the ELF_π and ELF_σ components. The isosurface for ELF_σ for B_{12} is separated into three reducible basins having each a bifurcation value of 0.87. The corresponding σ electrons are delocalized over the five-member ring. A higher value of 0.92 is found by separating completely the isosurface into irreducible basins, which leads to an assignment of σ aromaticity for the system. A bifurcation value of 0.88 is also found for ELF_π. We noted an important distribution in that electrons are delocalized within each of the five-membered rings for both ELF_π and ELF_σ isosurfaces, which ultimately results in the multiple aromaticity of B_{12}.

B_{13}. The structure, stability, and spectroscopic properties of B_{13} clusters have attracted much attention due to the high stability of the B_{13}^+ cation.[76] Two stable structures for B_{13} have been proposed: the quasi-planar **XXIV** (C_{2v}, $^2A_1$) and the convex **XXV** (C_{2v}, $^2B_1$) in which three hexagonal subunits are present.[4] A similar quasi-planar structure (C_s, $^2A'$) was also located,[16] but it is less stable than the two structures given above. We explored further the possible geometries for B_{13} and confirmed that the structures **XXIV** and **XXV** are essentially degenerate in energy and are the most stable isomers. **XXV** is 0.4−0.7 kcal/mol lower than **XIV**. The next lower-lying isomer is the high symmetry **XXVI** (D_{2h}, $^2B_{3u}$), at 5.0 kcal/mol higher in energy. Thus, B_{13} is characterized by significant structural fluctionality.

Attachment of one electron to the SOMOs of the different B_{13} isomers does not affect much their geometry (cf., Figure 2). However, a change in the energy ordering does occur. The high symmetry structure **XXIX** in its low spin state (D_{2h}, ^1A_g) becomes the lowest-lying form, and the two other structures **XXVII** and **XXVIII** have high spin, and are ~23−24 kcal/mol higher in energy (Table 2). In their previous study, Zhai et al.[16] reported that a C_s structure is the most stable, but we cannot locate such a structure.

The G3B3 value for the VDE(B_{13}^-) of 3.98 eV is larger than the experimental value of 3.78 eV,[16] consistent with the calculations of the VDE for other B_n clusters at this level. The adiabatic EA between B_{13} **XXIV** and B_{13}^- **XXIX** is 3.62 eV. The adiabatic detachment energy of the anion from B_{13}^- **XXIX** to B_{13} **XXVI** is 3.81 eV. The latter value agrees well with the experimental result of 3.78 ± 0.02 eV.[16]

Zhai et al.[16] stated that as the B_{13}^- anion possesses eight electrons, it is π antiaromatic according to the Hückel rule. In contrast, Aihara et al.[29] suggested that the B_{13}^- anion is actually aromatic with a large positive resonance energy. Our ELF plots concur rather with the former view. The bifurcation value of ELF_π is found to be 0.65, which is low and makes B_{13}^- a globally π antiaromatic species. However, partial π electron delocalization can be identified in the anion over the three- and four-membered rings. The value of ELF_σ of 0.89 is high enough to suggest that the B_{13}^- anion has σ aromaticity. We thus assign B_{13}^- as being globally σ aromatic with islands of π aromaticity.

Binding Energies. To probe further the thermodynamic stability of the boron clusters, we now examine the binding

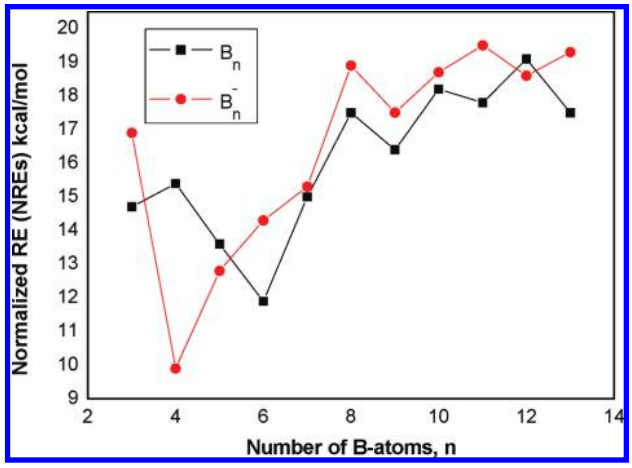

Figure 7. Size dependence of the normalized resonance energies (NRE in kcal/mol) of B_n and B_n^- clusters. Values obtained from G3B3 heats of formation at 0 K.

energy (D_e) and average binding energy (E_b)[77] defined as follows:

$$D_e(B_n) = \Delta H_f(B_{n-1}) + \Delta H_f(B) - \Delta H_f(B_n) \quad (4a)$$

$$D_e(B_n^-) = \Delta H_f(B_{n-1}^-) + \Delta H_f(B) - \Delta H_f(B_n^-) \quad (4b)$$

$$E_b(B_n) = [n\Delta H_f(B) - \Delta H_f(B_n)]/n = TAE/n \quad (5a)$$

$$E_b(B_n^-) = [(n)\Delta H_f(B) + \Delta H_f(e) - \Delta H_f(B_n^-)]/n \quad (5b)$$

where $\Delta H_f(e)$ is set equal to zero. The D_e corresponds to a dissociation energy, which is the energy required to remove one B atom from a cluster, and the E_b is the average energy of stabilization per atom in the cluster. The evolution of the quantities D_e and E_b with respect to n is shown in Table 6 and Figures 4 and 5. The experimental D_e is the heat of atomization of B, which is 5.86 eV at 0 K.[78]

E_b essentially increases as a function of n. The evolution of E_b is nearly parallel for both neutral and anionic forms (Figure 4). It grows rapidly in small-sized clusters (n from 2 to 6), but the rate becomes smaller from $n = 7$, and then the quantity varies more smoothly and tends to approach the asymptote limit value of the D_e slowly (for $n = 13$, E_b being ~4.6 eV for the neutral and ~5 eV for the anion). Note that in the series of $B_nH_n^{2-}$ dianions with $n = 5-12$, the energy per BH-group was also found to linearly increase with respect to n.[79] The D_e is size-dependent and exhibits irregular oscillations for the smaller compounds (Figure 5). B_3^- is thus the most stable and B_4 the least stable cluster with respect to bond cleavage. Up to $n = 10$, there is a nearly parallel evolution of BEs in both neutral and anionic systems, where within each of the pairs B_8/B_8^-, B_9/B_9^-, and B_{10}/B_{10}^-, the neutral and anionic forms have nearly the same BE values. An odd−even alternation begins at $n = 11$, where a closed-shell species is more stable than an open-shell counterpart. The clusters B_{11}^-, B_{12}, and B_{13}^-, having each an even number of electrons, are thus more stable and expected to be associated with higher abundance in, for example, a mass spectrum recording their formation.

Table 7 lists the calculated energies of the condensation processes involving the addition of a B_2, B_3, or B_4 unit. The condensation reactions are substantially exothermic ranging from −90 to −230 kcal/mol and do not exhibit any obvious patterns.

Resonance Energies. In our previous study,[30] we considered the resonance energy (RE)[48,80] defined by eqs 6:

$$RE(B_n) = \Delta E(B_n \rightarrow nB) - m\Delta E(B_2 \rightarrow nB) = TAE(B_n) - mTAE(B_2) \quad (6a)$$

$$RE(B_n^-) = \Delta E(B_n \rightarrow nB) - (m-1)\Delta E(B_2 \rightarrow nB) - \Delta E(B_2^- \rightarrow 2B + e) \quad (6b)$$

in which the diatomic B_2 can be in either the $^1\Sigma_g^+$ or the $^3\Sigma_g^-$ state, and m is the number of BB bonds in B_n. The REs evaluated as a function of m are given in Table 8, and their evolution is shown in Figure 6. Taking the singlet state for B_2 and assuming $m = 3, 5, 7$ for B_3^-, B_4, and B_5^-, the REs amount to 111, 62, and 146 kcal/mol, respectively. For larger clusters, the determination of the number of effective BB bonds becomes more difficult. For B_6, there are arguments as to whether to assign m being either 8 or 9. For B_{12}, m could be taken as 21 (each additional B bringing in two bonds) or 24 (number of BB bonds being counted from structure **XXII** ($^1A_1$)). This leads to the RE values of 230 ($m = 21$) and 78 ($m = 24$) kcal/mol. The merit of this parameter is that its emphasizes the enormous excess energy brought about following a clustering of elements, with respect to a simple combination of BB bond energies.

The normalized resonance energy is defined as NRE = RE/n, and thus describes the amount of resonance energy per atom, which may be a more convenient index to quantify the electron delocalization. The calculated values are listed in Table 8, and their variations are illustrated in Figure 7. For the boron clusters, the NRE values range from 9 to 20 kcal/mol; the larger is the NRE, the more stabilized is the cluster. For example, B_3^- is more stabilized than B_3, B_4 more stabilized than B_4^-, and B_3^- more stabilized than B_4. A species having an even number of electrons (such as B_6, B_8, B_{10}) does not necessarily possess a larger NRE than its odd number counterpart. The clusters B_8^-, B_9^-, B_{10}^-, B_{11}^-, B_{12}, and B_{13}^- have comparable NRE values.

Conclusions

In the present theoretical study, thermochemical properties of a series of small boron clusters B_n ($n = 5-13$) and their anions B_n^- were calculated by using both the composite CCSD(T)/CBS (for $n = 5-9$) and the G3B3 methods. As far as we are aware, no experimental heats of formation are available for comparison. For the adiabatic electron affinities (AEA) and vertical electron detachment energies (VDE), where the whole set of photoelectron data was reported, there is a reasonable agreement with the G3B3 method tending to overestimate the EAs and VDEs by about 0.2 eV unless there is spin contamination. The B_6/B_6^- pair represents a case where the UHF wave functions are strongly spin-contaminated, and thus UHF-based methods (such as G3B3) cannot be used for quantitative predictions. For some clusters, the lowest energy anionic cluster may not have the same geometry as the lowest energy neutral cluster so the adiabatic detachment energy does not correspond to the global EA. The global energy minima of the boron clusters considered agree with previous predictions except for B_8 where the high symmetry high spin state $^3A_2'$, D_{7h} is predicted to be the ground electronic state.

Use of a topological analysis of the electron localization function, in particular a partition of the global electronic density into σ and π components, provides additional insights into the aromaticity of boron clusters. The global aromaticity of these clusters obeys the conventional Hückel rule, and, in some cases, the analysis emphasizes the role of partially delocalized electrons in a nonaromatic environment. The larger clusters appear to have multiple aromaticity.[48]

The evolution of the average binding energies (energy per atom) is nearly parallel for both neutral and anionic series, and they tend to approach the asymptote of the heat of atomization of the elemental boron in the solid state. The resonance energies, as defined from the TAEs, and in particular the normalized resonance energies are convenient indices to quantify the stabilization of a cluster by electron delocalization. Finally, the evolution of the geometry and resonance energy (through the parameter *m*) suggests that the boron cluster grows in such a way that each additional B atom brings about two (for small clusters) or three (for larger clusters) new BB bonds, and forms planar or nearly planar rings with high symmetry. There is a preference for low spin electronic state.

Acknowledgment. Funding was provided in part by the Department of Energy, Office of Energy Efficiency and Renewable Energy under the Hydrogen Storage Grand Challenge, Solicitation No. DE-PS36-03GO93013. This work was done as part of the Chemical Hydrogen Storage Center. D.A.D. is indebted to the Robert Ramsay Endowment of the University of Alabama. M.T.N. thanks the K.U. Leuven Research Council for support (GOA, IDO, and IUAP programs) and Dr. B. Kiran for valuable discussion on B_{12}. T.B.T. thanks the Arenberg Doctoral School for a scholarship.

Supporting Information Available: Tables containing the Cartesian coordinates for optimized geometries, CCSD(T)/aug-cc-pV*n*Z total energies, MP2/aVDZ vibrational frequencies, and G3B3 total energies and TAEs. This material is available free of charge via the Internet at http://pubs.acs.org.

References and Notes

(1) (a) Hanley, L.; Anderson, S. L. *J. Chem. Phys.* **1988**, *89*, 2848. (b) Hanley, L.; Whitten, J. L.; Anderson, S. L. *J. Chem. Phys.* **1988**, *92*, 5803. (c) Hintz, P. A.; Ruatta, S. A.; Anderson, S. L. *J. Chem. Phys.* **1990**, *92*, 292. (d) Hintz, P. A.; Ruatta, S. A.; Anderson, S. L. *J. Chem. Phys.* **1991**, *94*, 6446. (e) Smolanoff, J.; Lapicki, A.; Kline, N.; Anderson, S. L. *J. Phys. Chem.* **1995**, *99*, 16276. (f) Peiris, D.; Lapicki, A.; Anderson, S. L.; Napora, R.; Linder, D.; Page, M. *J. Phys. Chem. A* **1997**, *101*, 9935. (g) Lapicki, A.; Peiris, D.; Anderson, S. L. *J. Phys. Chem. A* **1999**, *103*, 226.

(2) (a) Kato, H.; Tanaka, E. *J. Comput. Chem.* **1991**, *12*, 1097. (b) Kato, H.; Yamashita, K.; Morokuma, K. *Chem. Phys. Lett.* **1992**, *190*, 361.

(3) Ray, A. K.; Howard, I. A.; Kanal, K. M. *Phys. Rev. B* **1992**, *45*, 14247.

(4) Boustani, I. *Phys. Rev. B* **1997**, *55*, 16426.

(5) Bonacic-Koutecky, V.; Fantucci, P.; Koutecky, J. *Chem. Rev.* **1991**, *91*, 1035.

(6) (a) Zubarev, D. Y.; Boldyrev, A. I. *J. Comput. Chem.* **2006**, *28*, 251. (b) Rincon, L.; Almeida, R.; Alvarellos, J. E.; Garcia-Aldea, D.; Hasmy, A.; Gonzalez, C. *Dalton Trans.* **2009**, 3328.

(7) Li, Q.; Zhao, Yi.; Xu, W.; Li, N. *Int. J. Quantum Chem.* **2004**, *101*, 219.

(8) Drummond, M. L.; Meunier, V.; Sumpter, B. G. *J. Phys. Chem. A* **2007**, *111*, 6539.

(9) Tanimoto, M.; Saito, S.; Hirota, E. *J. Chem. Phys.* **1986**, *84*, 1210.

(10) (a) Burkholder, T. R.; Andrews, L. *J. Chem. Phys.* **1991**, *95*, 8697. (b) Maki, A. G.; Burkholder, J. B.; Sinha, A.; Howard, C. J. *J. Mol. Spectrosc.* **1988**, *130*, 238.

(11) (a) Green, G. J.; Gole, J. L. *Chem. Phys. Lett.* **1980**, *69*, 45. (b) Gole, J. L.; Ohllson, B.; Green, G. *Chem. Phys.* **2001**, *273*, 59.

(12) Ruscic, B. M.; Curtius, L. A.; Berkowitz, J. *J. Chem. Phys.* **1984**, *80*, 3962.

(13) Wenthold, P. G.; Kim, J. B.; Jonas, K. L.; Lineberger, W. C. *J. Phys. Chem. A* **1997**, *101*, 4472.

(14) Li, S. D.; Zhai, H. J.; Wang, L. S. *J. Am. Chem. Soc.* **2008**, *130*, 2753.

(15) Atis, M.; Ozdogan, C. *Int. J. Quantum Chem.* **2007**, *107*, 729.

(16) Zhai, H. J.; Wang, L. S.; Zubarev, D. Y.; Boldyrev, A. I. *J. Phys. Chem. A* **2006**, *110*, 1689.

(17) (a) La Placa, S. J.; Roland, P. A.; Wynne, J. J. *Chem. Phys. Lett.* **1992**, *190*, 163. (b) Roland, P. A.; Wynne, J. J. *J. Chem. Phys.* **1993**, *99*, 8599.

(18) Feng, X. J.; Lou, Y. H. *J. Phys. Chem. A* **2007**, *111*, 2420.

(19) Yang, Z.; Yan, Y. L.; Zhao, W. J.; Lei, X. L.; Ge, G. X.; Lou, Y. H. *Acta Phys. Sin.* **2007**, *56*, 2590.

(20) Wang, R. X.; Zhang, D. J.; Zhu, R. X.; Liu, C. B. *J. Mol. Struct. (THEOCHEM)* **2007**, *822*, 119.

(21) (a) Cabria, I.; Lopez, M. J.; Alonso, J. A. *Nanotechnology* **2006**, *17*, 778. (b) Wu, G.; Wang, J.; Zhang, X.; Zhu, L. *J. Phys. Chem. C* **2009**, *113*, 7052.

(22) Quandt, A.; Boustani, I. *ChemPhysChem* **2005**, *6*, 2001.

(23) (a) Gopakumar, G.; Nguyen, M. T.; Ceulemans, A. *Chem. Phys. Lett.* **2008**, *450*, 175. (b) Gopakumar, G.; Nguyen, M. T.; Ceulemans, A. *Chem. Phys. Lett.* **2008**, 46126.

(24) (a) Boustani, I. *Int. J. Quantum Chem.* **1994**, *52*, 1081. (b) Boustani, I. *Chem. Phys. Lett.* **1995**, *233*, 273. (c) Boustani, I. *Chem. Phys. Lett.* **1995**, *240*, 135.

(25) Alexandrova, A. N.; Boldyrev, A. I.; Zhai, H. J.; Wang, L. S. *Coord. Chem. Rev.* **2006**, *250*, 2811.

(26) Zhai, H. J.; Kiran, B.; Li, J.; Wang, L. S. *Nat. Mater.* **2003**, *2*, 827.

(27) Zhai, H. J.; Alexandrova, A. N.; Birch, K. A.; Boldyrev, A. I.; Wang, L. S. *Angew. Chem., Int. Ed.* **2003**, *42*, 6004.

(28) Sergeeva, A. P.; Zubarev, D. Y.; Zhai, H. J.; Boldyrev, A. I.; Wang, L. S. *J. Am. Chem. Soc.* **2008**, *130*, 7244.

(29) Aihara, J. I.; Kanno, H.; Ishida, T. *J. Am. Chem. Soc.* **2005**, *127*, 13324.

(30) Nguyen, M. T.; Matus, M. H.; Ngan, V. T.; Grant, D. J.; Dixon, D. A. *J. Phys. Chem. A* **2009**, *113*, 4895.

(31) Frisch, M. J.; Trucks, G. W.; Schlegel, H. B.; Scuseria, G. E.; Robb, M. A.; Cheeseman, J. R.; Montgomery, J. A., Jr.; Vreven, T.; Kudin, K. N.; Burant, J. C.; Millam, J. M.; Iyengar, S. S.; Tomasi, J.; Barone, V.; Mennucci, B.; Cossi, M.; Scalmani, G.; Rega, N.; Petersson, G. A.; Nakatsuji, H.; Hada, M.; Ehara, M.; Toyota, K.; Fukuda, R.; Hasegawa, J.; Ishida, M.; Nakajima, T.; Honda, Y.; Kitao, O.; Nakai, H.; Klene, M.; Li, X.; Knox, J. E.; Hratchian, H. P.; Cross, J. B.; Bakken, V.; Adamo, C.; Jaramillo, J.; Gomperts, R.; Stratmann, R. E.; Yazyev, O.; Austin, A. J.; Cammi, R.; Pomelli, C.; Ochterski, J. W.; Ayala, P. Y.; Morokuma, K.; Voth, G. A.; Salvador, P.; Dannenberg, J. J.; Zakrzewski, V. G.; Dapprich, S.; Daniels, A. D.; Strain, M. C.; Farkas, O.; Malick, D. K.; Rabuck, A. D.; Raghavachari, K.; Foresman, J. B.; Ortiz, J. V.; Cui, Q.; Baboul, A. G.; Clifford, S.; Cioslowski, J.; Stefanov, B. B.; Liu, G.; Liashenko, A.; Piskorz, P.; Komaromi, I.; Martin, R. L.; Fox, D. J.; Keith, T.; Al-Laham, M. A.; Peng, C. Y.; Nanayakkara, A.; Challacombe, M.; Gill, P. M. W.; Johnson, B.; Chen, W.; Wong, M. W.; Gonzalez, C.; Pople, J. A. *Gaussian 03*, revision C.01; Gaussian, Inc.: Wallingford, CT, 2004.

(32) Werner, H.-J.; Knowles, P. J.; Amos, R. D.; Bernhardsson, A.; Berning, A.; Celani, P.; Cooper, D. L.; Deegan, M. J. O.; Dobbyn, A. J.; Eckert, F.; Hampel, C.; Hetzer, G.; Korona, T.; Lindh, R.; Lloyd, A. W.; McNicholas, S. J.; Manby, F. R.; Meyer, W.; Mura, M. E.; Nicklass, A.; Palmieri, P.; Pitzer, R. M.; Rauhut, G.; Schütz, M.; Stoll, H.; Stone, A. J.; Tarroni, R.; Thorsteinsson, T. *MOLPRO-2002, a package of initio programs*; Universität Stüttgart: Stüttgart, Germany; University of Birmingham: Birmingham, United Kingdom, 2002.

(33) (a) Peterson, K. A.; Xantheas, S. S.; Dixon, D. A.; Dunning, T. H., Jr. *J. Phys. Chem. A* **1998**, *102*, 2449. (b) Feller, D.; Peterson, K. A. *J. Chem. Phys.* **1998**, *108*, 154. (c) Dixon, D. A.; Feller, D. *J. Phys. Chem. A* **1998**, *102*, 8209. (d) Feller, D.; Peterson, K. A. *J. Chem. Phys.* **1999**, *110*, 8384. (e) Feller, D.; Dixon, D. A. *J. Phys. Chem. A* **1999**, *103*, 6413. (f) Feller, D. *J. Chem. Phys.* **1999**, *111*, 4373. (g) Feller, D.; Dixon, D. A. *J. Phys. Chem. A* **2000**, *104*, 3048. (h) Feller, D.; Sordo, J. A. *J. Chem. Phys.* **2000**, *113*, 485. (i) Feller, D.; Dixon, D. A. *J. Chem. Phys.* **2001**, *115*, 3484. (j) Dixon, D. A.; Feller, D.; Sandrone, G. *J. Phys. Chem. A* **1999**, *103*, 4744. (k) Ruscic, B.; Wagner, A. F.; Harding, L. B.; Asher, R. L.; Feller, D.; Dixon, D. A.; Peterson, K. A.; Song, Y.; Qian, X.; Ng, C.; Liu, J.; Chen, W.; Schwenke, D. W. *J. Phys. Chem. A* **2002**, *106*, 2727. (l) Feller, D.; Dixon, D. A.; Peterson, K. A. *J. Phys. Chem. A* **1998**, *102*, 7053. (m) Dixon, D. A.; Feller, D.; Peterson, K. A. *J. Chem. Phys.* **2001**, *115*, 2576.

(34) (a) Curtiss, L. A.; Raghavachari, K.; Redfern, P. C.; Rassolov, V.; Pople, J. A. *J. Chem. Phys.* **1998**, *109*, 7764. (b) Baboul, A. G.; Curtiss, L. A.; Redfern, P. C. *J. Chem. Phys.* **1999**, *110*, 7650.

(35) Bartlett, R. J.; Musial, M. *Rev. Mod. Phys* **2007**, *79*, 291, and references therein.

(36) (a) Dunning, T. H. *J. Chem. Phys.* **1989**, *90*, 1007. (b) Kendell, R. A.; Dunning, T. H.; Harrison, R. J. *J. Chem. Phys.* **1992**, *96*, 6796.

(37) Rittby, M.; Bartlett, R. J. *J. Phys. Chem.* **1988**, *92*, 3033.
(38) Knowles, P. J.; Hampel, C.; Werner, H.-J. *J. Chem. Phys.* **1994**, *99*, 5219.
(39) Deegan, M. J. O.; Knowles, P. J. *Chem. Phys. Lett.* **1994**, *227*, 321.
(40) Peterson, K. A.; Woon, D. E.; Dunning, T. H., Jr. *J. Chem. Phys.* **1994**, *100*, 7410.
(41) (a) Helgaker, T.; Klopper, W.; Koch, H.; Nagel, J. *J. Chem. Phys.* **1997**, *106*, 9639. (b) Halkier, A.; Helgaker, T.; Jørgensen, P.; Klopper, W.; Koch, H.; Olsen, J.; Wilson, A. K. *Chem. Phys. Lett.* **1998**, *286*, 243.
(42) (a) Douglas, M.; Kroll, N. M. *Ann. Phys.* **1974**, *82*, 89–155. (b) Hess, B. A. *Phys. Rev. A* **1985**, *32*, 756–763. (c) Hess, B. A. *Phys. Rev. A* **1986**, *33*, 3742–3748.
(43) de Jong, W. A.; Harrison, R. J.; Dixon, D. A. *J. Chem. Phys.* **2001**, *114*, 48.
(44) EMSL basis set library. http://www.emsl.pnl.gov/forms/basisform.html.
(45) Moore, C. E. *Atomic Energy Levels as Derived from the Analysis of Optical Spectra, Volume 1, H to V*; U.S. National Bureau of Standards Circular 467, U.S. Department of Commerce; National Technical Information Service, COM-72-50282: Washington, D.C., 1949.
(46) Karton, A.; Martin, J. M. L. *J. Phys. Chem. A* **2007**, *111*, 5936.
(47) Curtiss, L. A.; Raghavachari, K.; Redfern, P. C.; Pople, J. A. *J. Chem. Phys.* **1997**, *106*, 1063.
(48) Zhan, C. G.; Zheng, F.; Dixon, D. A. *J. Am. Chem. Soc.* **2002**, *124*, 14795.
(49) Becke, A.; Edgecombe, K. *J. Chem. Phys.* **1990**, *92*, 5397.
(50) (a) Silvi, B.; Savin, A. *Nature* **1994**, *371*, 683. (b) Savin, A.; Becke, A.; Flad, D.; Nesper, R.; Preuss, H.; Schnering, H. V. *Angew. Chem., Int. Ed. Engl.* **1991**, *30*, 409. (c) Savin, A.; Silvi, B.; Colonna, F. *Can. J. Chem.* **1996**, *74*, 1088.
(51) Santos, J. C.; Tiznado, W.; Contreras, R.; Fuentealba, P. *J. Chem. Phys.* **2004**, *120*, 1670.
(52) (a) Noury, S.; Krokidis, X.; Fuster, F.; Silvi, B. *TOPMOD Package*; Universite Pierre et Marie Curie: Paris, 1997. (b) Noury, S.; Krokidis, X.; Fuster, F.; Silvi, B. *Comput. Chem. (Oxford)* **1999**, *23*, 597.
(53) Kohout, M. *DGrid, version 2.3*; Max-Planck-Institut fur Chemische Physik fester Stoffe: Dresden, Germany, 2001.
(54) (a) Laaksonen, L. *J. Mol. Graph.* **1992**, *10*, 33. (b) Bergman, D. L.; Laaksonen, L.; Laaksonen, A. *J. Mol. Graphics Model.* **1997**, *15*, 301.
(55) Chase, M. W. *J. Phys. Chem. Ref. Data, Monogr.* **1998**, *9*, 1–957.
(56) Li, Q. S.; Jin, H. W. *J. Phys. Chem. A* **2002**, *106*, 7042.
(57) Zhai, H. J.; Wang, L. S.; Alexandrova, A. N.; Boldyrev, A. I. *J. Chem. Phys.* **2002**, *117*, 7917.
(58) Ricca, A.; Bauschlicher, C. W. *Chem. Phys.* **1996**, *208*, 233.
(59) Niu, J.; Rao, B. K.; Jena, B. *J. Chem. Phys.* **1997**, *107*, 132.
(60) Whiteside, R. A. Ph.D. Thesis, Carnegie Mellon University, Pittsburgh, PA, 1981.
(61) Li, Q. S.; Jin, Q.; Lou, Q.; Tang, A. C.; Yu, J. K.; Zhang, H. X. *Int. J. Quantum Chem.* **2003**, *94*, 269.
(62) Ma, J.; Li, Z.; Fan, K.; Zhou, M. *Chem. Phys. Lett.* **2003**, *372*, 708.
(63) Alexandrova, A. N.; Boldyrev, A. I.; Zhai, H. J.; Wang, L. S.; Steiner, E.; Fowler, P. W. *J. Phys. Chem. A* **2003**, *107*, 1359.
(64) Alexandrova, A. N.; Boldyrev, A. I.; Zhai, H. J.; Wang, L. S. *J. Phys. Chem. A* **2004**, *108*, 3509.
(65) Li, Q. S.; Gong, L. F.; Gao, Z. M. *Chem. Phys. Lett.* **2004**, *390*, 220.
(66) Reis, H.; Papadopoulos, M. G.; Boustani, I. *Int. J. Quantum Chem.* **2002**, *78*, 131.
(67) Boustani, I. *Phys. Rev. B* **1997**, *55*, 16426.
(68) Li, Q. S.; Zhao, Y.; Xu, W.; Li, N. *Int. J. Quantum Chem.* **2005**, *101*, 219.
(69) Bonacic-Koutecky, V.; Fantucci, P.; Koutecky, J. *Chem. Rev.* **1991**, *91*, 1035.
(70) Zhai, H. J.; Alexandrova, A. N.; Birch, K. A.; Boldyrev, A. I.; Wang, L. S. *Angew. Chem., Int. Ed.* **2003**, *42*, 6004.
(71) Cao, P. L.; Zhao, W.; Li, B. X.; Song, B.; Zhou, X. Y. *J. Phys: Condens. Matter.* **2001**, *13*, 5065.
(72) Satpati, P.; Sebastian, K. L. *J. Mol. Struct. (THEOCHEM)* **2007**, *823*, 74.
(73) Lau, K. C.; Deshpande, M.; Pandey, R. *Int. J. Quantum Chem.* **2005**, *102*, 656.
(74) Satpati, P.; Sebastian, K. L. *J. Mol. Struct. (THEOCHEM)* **2007**, *823*, 74.
(75) Lau, K. C.; Deshpande, M.; Pandey, R. *Int. J. Quantum Chem.* **2005**, *102*, 656.
(76) (a) Kawai, R.; Weare, J. *Chem. Phys. Lett.* **1992**, *191*, 311. (b) Fowler, J. E.; Ugalde, J. M. *J. Phys. Chem. A* **2000**, *104*, 397. (c) Aihara, J. *J. Phys. Chem. A* **2001**, *105*, 5486.
(77) Ngan, V. T.; De Haeck, J.; Le, H. T.; Gopakumar, G.; Lievens, P.; Nguyen, M. T. *J. Phys. Chem. A* **2009**, *113*, 9080, and references therein.
(78) Kittel, C. *Introduction to Solid State Physics*, 7th ed.; Wiley: New York, 1996.
(79) Nguyen, M. T.; Matus, M. H.; Dixon, D. A. *Inorg. Chem.* **2007**, *46*, 7561.
(80) Dewar, M. J. S.; Deal Lano, C. *J. Am. Chem. Soc.* **1969**, *91*, 789.

JP9085848